AD NUMBER
ADB006102
LIMITATION CHANGES

TO:

Approved for public release; distribution is unlimited. Document partially illegible.

FROM:

Distribution authorized to U.S. Gov't. agencies only; Test and Evaluation; NOV 1974. Other requests shall be referred to Air Force Armament Laboratory, DLMM, Eglin AFB, FL 32542.

AUTHORITY

afatl ltr, 29 mar 1977

PHASED ARRAY ANTENNA

AND

RADIOMETRY DEVELOPMENT

**AIR-TO-SURFACE WEAPONS BRANCH
GUIDED WEAPONS DIVISION**

NOVEMBER 1974

D D C

AUG 27 1975

D

FINAL REPORT: January 1973 to June 1974

AIR FORCE ARMAMENT LABORATORY

AIR FORCE SYSTEMS COMMAND • UNITED STATES AIR FORCE

EGLIN AIR FORCE BASE, FLORIDA

SECURITY CLASSIFICATION OF THIS PAGE *(When Data Entered)*

REPORT DOCUMENTATION PAGE		READ INSTRUCTIONS BEFORE COMPLETING FORM
1. REPORT NUMBER AFATL-TR-74-192	2. GOVT ACCESSION NO.	3. RECIPIENT'S CATALOG NUMBER
4. TITLE *(and Subtitle)* PHASED ARRAY ANTENNA AND RADIOMETRY DEVELOPMENT		5. TYPE OF REPORT & PERIOD COVERED Final Report January 1973 - June 1974
		6. PERFORMING ORG. REPORT NUMBER
7. AUTHOR(s) Franklin Prestwood John Hilburn		8. CONTRACT OR GRANT NUMBER(s) F08635-73-C-0048
9. PERFORMING ORGANIZATION NAME AND ADDRESS Guided Weapons Division (DLMM) Air Force Armament Laboratory Eglin Air Force Base, Florida 32542		10. PROGRAM ELEMENT, PROJECT, TASK AREA & WORK UNIT NUMBERS Project 670B
11. CONTROLLING OFFICE NAME AND ADDRESS Air Force Armament Laboratory Air Force Systems Command Eglin Air Force Base, Florida 32542		12. REPORT DATE November 1974
		13. NUMBER OF PAGES
14. MONITORING AGENCY NAME & ADDRESS(If different from Controlling Office)		15. SECURITY CLASS. (of this report) UNCLASSIFIED
		15a. DECLASSIFICATION DOWNGRADING SCHEDULE

16. DISTRIBUTION STATEMENT *(of this Report)*

Distribution limited to U. S. Government agencies only; this report documents test and evaluation; distribution limitation applied November 1974. Other requests for this docuemnt must be referred to the Air Force Armament Laboratory (DLMM), Eglin Air Force Base, Florida 32542.

17. DISTRIBUTION STATEMENT *(of the abstract entered in Block 20, if different from Report)*

D D C

AUG 27 1975

18. SUPPLEMENTARY NOTES

Available in DDC.

19. KEY WORDS *(Continue on reverse side if necessary and identify by block number)*
Bomb Guidance System
Radiometric Seeker Development
Phased Array Antenna
Flight Test
Tower Test

20. ABSTRACT *(Continue on reverse side if necessary and identify by block number)*
This report describes the flight tests performed for a radiometric bomb guidance system developed by Martin-Marietta Corp., Orlando, Florida. The preliminary system evaluations prior to the joint USAF-Navy flight tests at Santa Ana, California are discussed and the results of these initial tests are presented. The modification of the frequency-scanned radiometric bomb guidance system is then described. For this modified system (the dual-beam frequency-scanned radiometer) the development of the circuitry for a stairstep mode and a ramp mode of operation is discussed. A dual-beam frequency-scarned antenna network

DD FORM 1473 EDITION OF 1 NOV 65 IS OBSOLETE
1 JAN 73

SECURITY CLASSIFICATION OF THIS PAGE *(When Data Entered)*

Item 20 Continued:

employing RG-52/U slotted waveguide is given, and the results from tower tests of the system are presented. Finally, an alternate system, a modified dual-beam frequency-scanned radiometer, is described. The range gate circuitry and a frequency-mechanically-scanned antenna are described. Preliminary tower test results are then given.
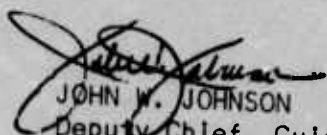
PREFACE

This report describes the results for a flight test program and a dual-beam frequency-scanned radiometer development under Project 670B and Contract F08635-73-C-0048 from 2 January 1973 to June 1974. The work was performed as a joint in-house effort between the Air Force Armament Laboratory and the Louisiana State University at Baton Rouge, Louisiana. The radiometric bomb guidance system was developed by the Martin-Marietta Corporation, Orlando, Florida, under Contract F08635-70-C-0126. The modification and the tower and flight testing of the first unit constructed was performed under Contract F08635-69-C-0142.

The program managers for the Air Force Armament Laboratory were Mr Franklin Prestwood and Captain Charles E. Brown. The project team leader from Louisiana State University was Dr John L. Hilburn, assisted by Dr Maurice Bouvier, Dr Paul M. Julich, and Mr Henry Arboneaux.

This technical report has been reviewed and is approved.

FOR THE COMMANDER

JOHN W. JOHNSON
Deputy Chief, Guided Weapons Division

TABLE OF CONTENTS

SECTION I

INTRODUCTION

1. BACKGROUND

A special one week flight test program involving a radiometric bomb seeker manufactured by the Martin-Marietta Corporation, Orlando, Florida, was conducted in the Kissimmee, Florida area during February 1973. The purpose of this test was to verify the airborne operational capability of the seeker (and the associated instrumentation) prior to the joint USAF/Navy helicopter flight test (Reference 1) which was conducted at Santa Ana, California from June through September 1973. The flight shakedown test was successful and only minor modifications were required prior to the helicopter flight test. The equipment also performed with 100% reliability during the helicopter flight test program.

The modification of the Frequency-Scanned Radiometric Bomb Guidance System was the continuation of a seeker concept being pursued by the Air Force Armament Laboratory and Louisiana State University. During recent years, two illumination aided radiometric techniques have been investigated for launch-leave-and-forget terminal guidance schemes for air-to-surface munitions; that is, a pulsed noise technique and a frequency modulated constant wave (FM/CW) technique. The radiometric bomb technique utilizes both pulsed noise and FM/CW schemes. A common pulsed frequency-scanned signal source is used to perform the following combined functions: (1) antenna steering, (2) illumination source, (3) receiver local oscillator source, and (4) pulsed gates for range gating and for time/spatial filtering.

2. OBJECTIVE

The near term objectives of this program were as follows:

(a) Verify the reliability of the radiometric bomb guidance system prior to investment in a large scale joint USAF/Navy flight test program.

(b) Continue development and perfection of the frequency-scanned radiometer.

Reference
1. Green, George M. Pulsed-Mode Microwave Radiometer Tracker Flight Test Report, Air Force Armament Laboratory TR-73-203. USAF Armament Laboratory, Eglin AFB, Florida. October 1973.

The long term objective of this program is to develop an all-weather millimeter-wave, terminal guidance concept for conventional air-to-surface munitions. Specific emphasis will be placed on combining the aerodynamic surfaces, such as canards, with the phased array antenna. The final objective is to reduce the overall munition cost, size, and weight so that the weapon may be deployed on a large scale basis against massive armor concentrations.

SECTION II

FLIGHT TESTS OF RADIOMETRIC BOMB GUIDANCE SYSTEM

The radiometric bomb guidance system discussed in this report was developed and constructed by the Martin-Marietta Corporation of Orlando, Florida (Reference 2). The modification and the tower and flight testing of the first unit constructed (Reference 3) was performed by personnel from the Air Force Armament Laboratory and Louisiana State University. The flight tests to be discussed in this section were performed in the Orlando, Florida, area for a second radiometer unit having performance characteristics superior to those of the first unit. At the conclusion of these tests, additional flight tests using a helicopter were performed for this unit (Reference 1).

1. RADIOMETRIC SYSTEM

A block diagram of the bomb guidance system is shown in Figure 1. The radiometer unit consists of a radiometric head (mounted in a Walleye gimbal) and a control panel console. The entire system was powered from a 24 volt battery with a 115V, 400 Hz inverter to provide power for the Walleye gimbal.

A block diagram of the video system employed in the tests is shown in Figure 2. This system consisted of a video recorder (Sony Model AV 3400), video monitor (Sony Model PVJ 3040), and a special function generator (Colorado Video X-Y Indicator-Model 621). The special function generator was used to generate a set of crosshairs on the video monitor, whose position was controlled by the azimuth and elevation error signals generated by the radiometer.

The complete system description and a detailed discussion of the modification necessary for flight testing are discussed in References 2 and 3, respectively.

2. FLIGHT TESTS

The flight tests for the radiometer bomb guidance system were performed in a low-wing, single-engine aircraft (Cherokee Six). This particular aircraft is identical to that employed in flight tests during prior programs (References 3 and 4). The equipment was mounted in the

---

Reference
2. Green, George M. Microwave Radiometric Terminal Guidance, Air Force Armament Laboratory TR-73-89. USAF Armament Laboratory, Eglin AFB, Florida. December 1973.
3. Hilburn, J. L. and F. H. Prestwood. Microwave Radiometric Measurement Program and Frequency Scanned Radiometer Development, Air Force Armament Laboratory TR-74-49. USAF Armament Laboratory, Eglin AFB, Florida. February 1974.

TV UNIT (EL to SPECIAL FUNCTION GENERATOR X-Y INDICATOR)
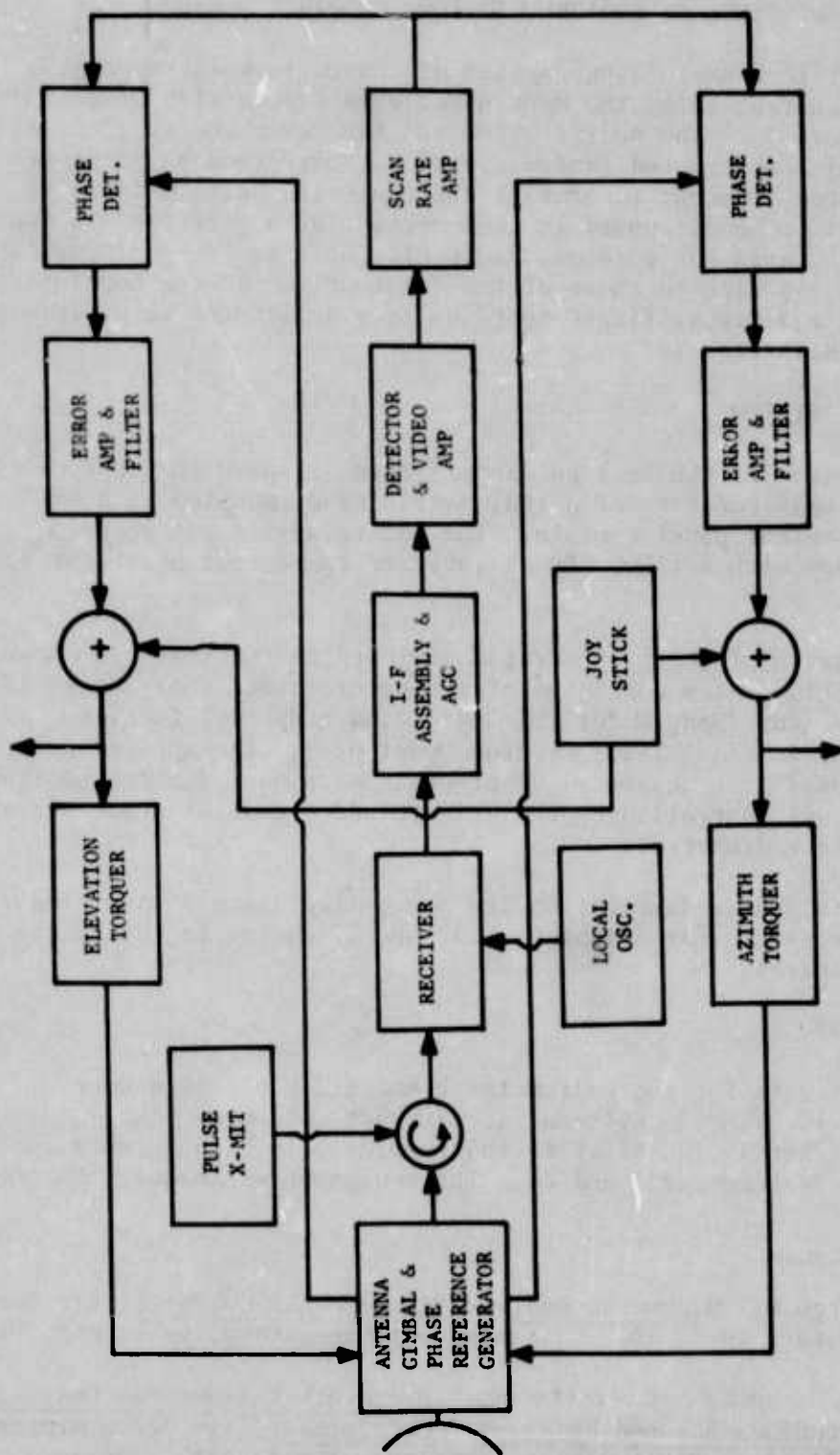
TV UNIT (AZ to SPECIAL FUNCTION GENERATOR X-Y INDICATOR)

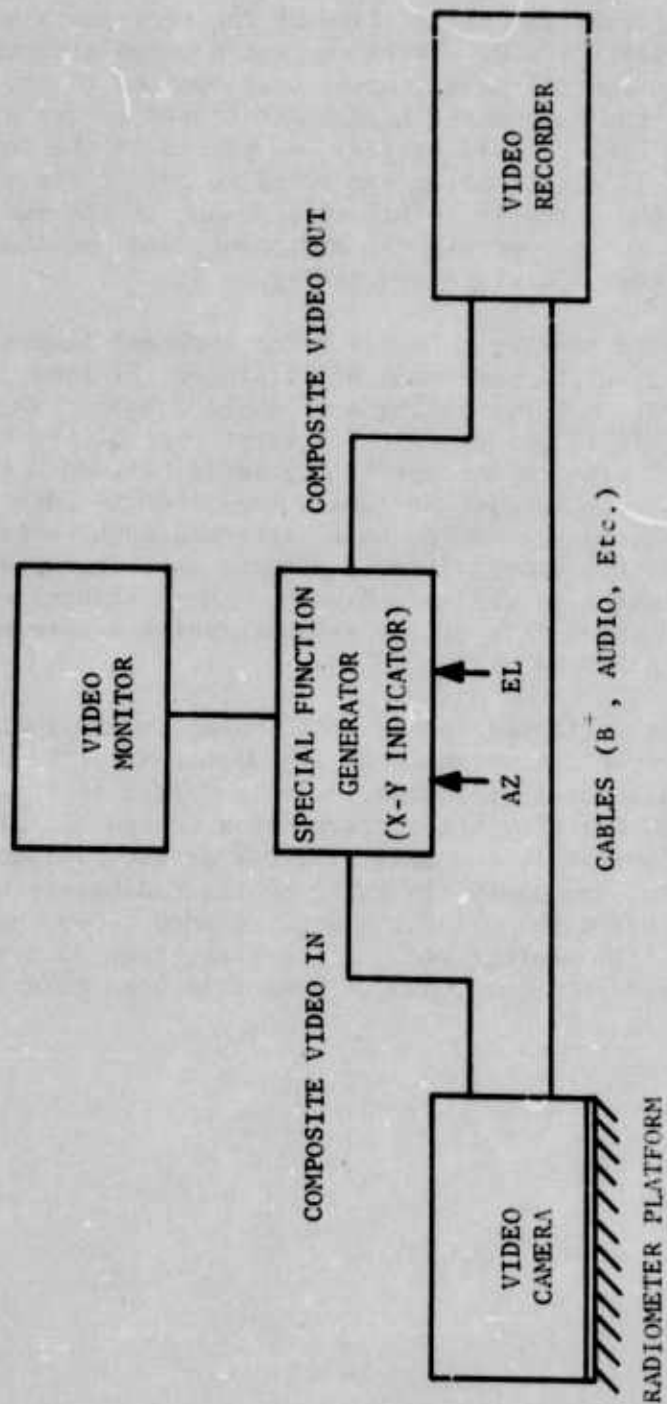Figure 1. Radiometric Bomb Guidance System.

8

Figure 2. Video System Employed in the Flight Tests.

9

fuselage of the aircraft in the position of the rear seats and the left center seat. The 115V, 400 Hz alternator was mounted directly behind the pilot seat, the control panel console was mounted in the center left seat position, and the radiometer head was fastened securely in the position of the rear seats. The 24 volt battery was placed in the forward luggage compartment to aid in distributing the total weight of the equipment (approximately 400 lb) in the aircraft. This arrangement of the equipment accommodated the pilot, a passenger to operate the equipment, and one observer. The deployment of the equipment is shown in Figure 3.

Flight tests were performed by Air Force Armament Laboratory and Louisiana State University personnel at Kissimmee, Florida, from 12 February to 16 February 1973. A total flying time of 17.2 hours was required for the performance of 12 flight tests. The first part of the tests involved the tracking of vehicles on Interstate Highway 4 between Orlando and Tampa, Florida. Vehicles were tracked at ranges from 1500 to 2000 feet. The receiver for the second radiometer unit performed much better than that of the first; however, the gimbal inertia effects which existed in the first unit were still present in the second unit. These effects were less severe, however, since the total mass of the antenna system was reduced in the construction of the second unit.

Tests were next performed for railway trains and railway yards. Also, flights were made over a test range at the Martin-Marietta Corporation plant and involved several test vehicles. The final test performed was an air-to-air test involving the tracking of a Cessna 105 aircraft that was flying at approximately the same altitude as the radiometer. In all the tests performed, successful tracking by the radiometer was demonstrated. Documentation was taken for all tests and included video tape, 16mm motion picture film, and 35mm photographs. Altogether, four 30 minute rolls of video tape and three 100 foot rolls of 16mm film were taken.

Reference
4. Hilburn, J. L., F. H. Prestwood and A. Mardon. Dual Frequency Radiometer, Air Force Armament Laboratory TR-71-100. USAF Armament Laboratory, Eglin AFB, Florida. August 1971.

(a) Outside View
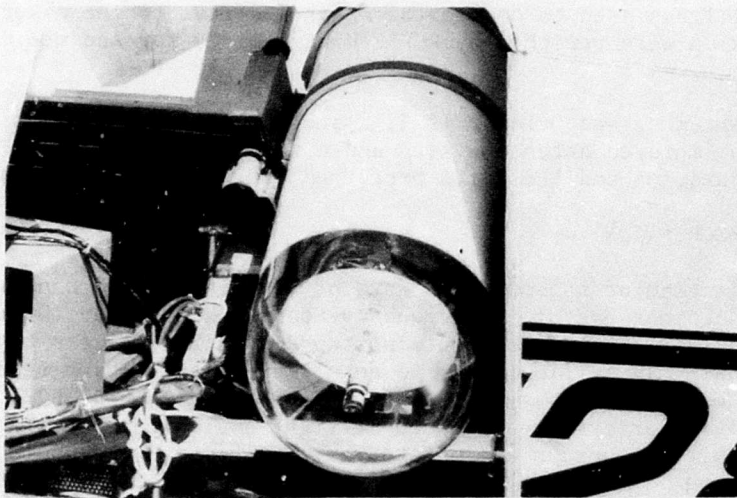
(b) Inside View

Figure 3.   Radiometer Equipment Installed for Flight Test.

11

SECTION III

MODIFICATION OF THE FREQUENCY-SCANNED RADIOMETRIC
BOMB GUIDANCE SYSTEM

This section describes a further development and modification of the Frequency-Scanned Active Radiometric Bomb Guidance System (Reference 3). When the work described in this section was initiated, the Frequency-Scanned Radiometric Bomb Guidance System was mounted on a finned, cylindrical aluminum structure which served as an M-84 bomb mock-up. This structure made it possible to simulate a method of mounting the four antenna arrays of the system on the fins of a bomb fuselage. Although this structure was appropriate for the initial tests, a more portable and more easily deployed form was desired for testing.

The evaluation of the Frequency-Scanned Radiometric System during 1973 and 1974 involved two distinct system configurations. The first configuration resulted when the aluminum bomb mock-up was eliminated as a mounting structure and was replaced by a 3 ft^2 plywood sheet. The resulting arrangement greatly simplified transportation of the system to Eglin AFB in June 1973, as well as facilitating deployment for testing. Furthermore, the system sensitivity was greatly improved because the long, rigid coaxial lines used to couple the antenna arrays to the mixer on the aluminum mock-up were replaced by RG-52/U waveguides for the new configuration.

During September and October 1973, a second configuration was designed to include an improved antenna system and a range gate network. This second configuration and the tests performed are described in Section IV.

1. SYSTEM DESCRIPTION

A block diagram of the modified form of the Frequency-Scanned Radiometric Bomb Guidance System, or Frequency-Scanned Radiometer (DBFSR), is shown in Figure 4. The system contains two distinct receivers that are used for scanning in an elevation and an azimuth plane. Each receiver has a 36 element waveguide array coupled to its mixer through RG-52/U waveguides. The two receiving arrays are oriented at right angles to each other, and the two transmitting arrays are mounted similarly (Figure 5). The same microwave source is used for generation of the transmitted power and the local oscillator power for the mixers. The third mixer, which is capped with a waveguide standard termination (Figure 4) acts as a reference source for the automatic gain control section. This channel provides a bias voltage that controls the gain of an i-f amplifier in each of the receiving channels.
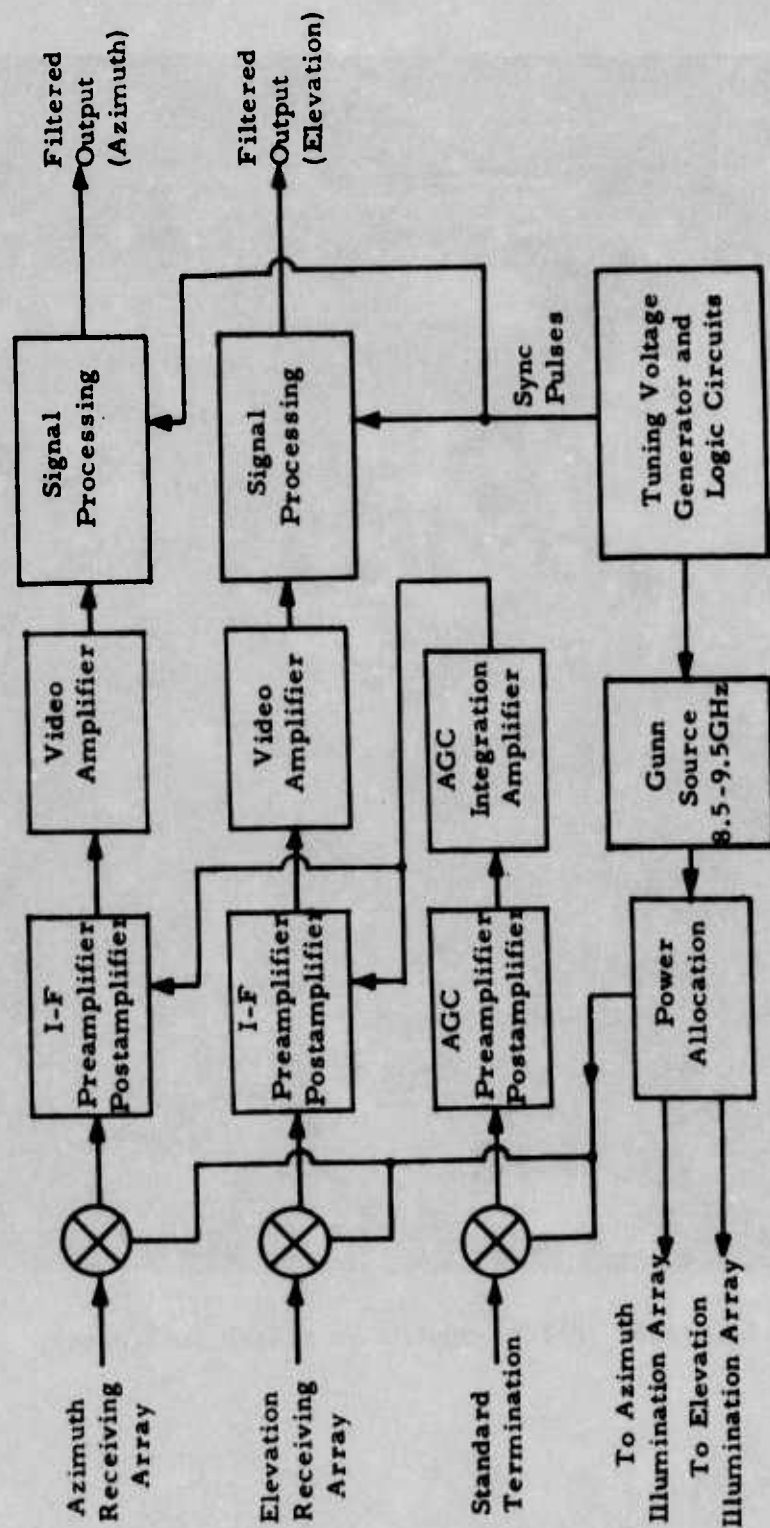
12

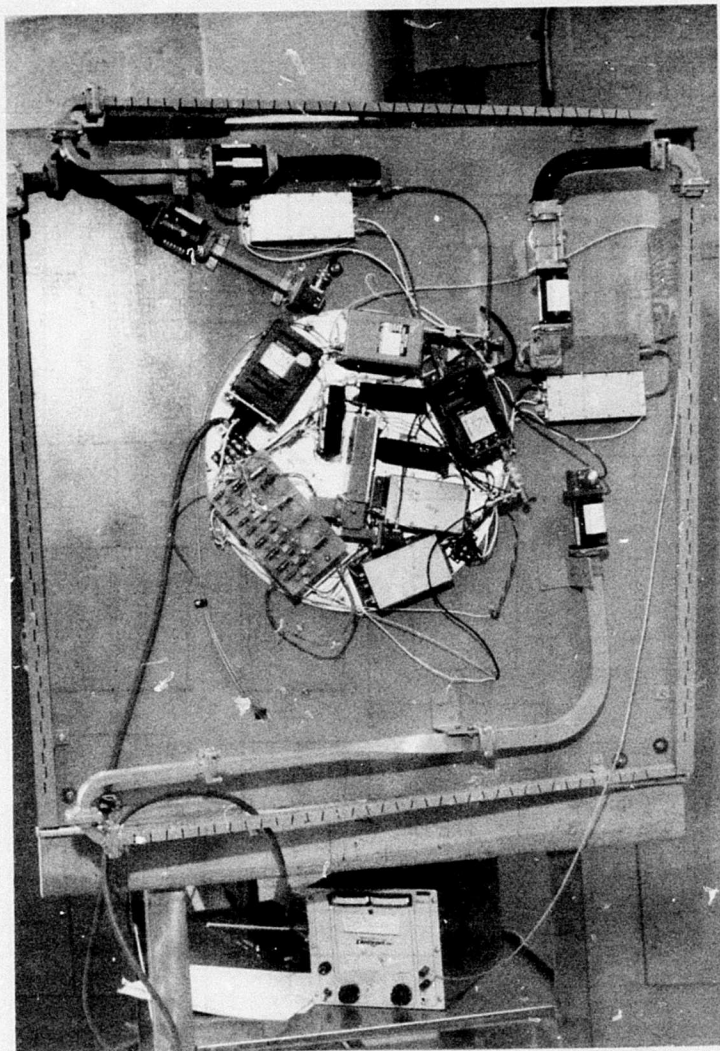Figure 4. Dual-Beam Frequency-Scanned Radiometer.

Figure 5. DBFSR Mounted on a Cart for Testing.

14

The antenna arrays used in the system are frequency scanned and were developed in a previous program (References 3 and 5). The angle of the array main beam is varied by changing the frequency of the local oscillator. The local oscillator is a varactor tuned microwave Gunn oscillator, which produces 100 mW of power from 8.5 to 9.5 GHz. The frequency is determined by the voltage present on the tuning voltage terminal of the device. The frequency variation that is necessary for scanning the array beams is obtained by applying a periodic waveform to the tuning voltage terminal, thus causing the frequency of the Gunn oscillator to vary according to the shape of the waveform. Two scanning methods were evaluated at Eglin AFB during June, July, and August 1973. Originally, a stairstep-shaped tuning voltage waveform was used to obtain a stepped scan. Later, the linear ramp tuning voltage was added in order to evaluate the performance of a continuous sweep method. Specially designed circuits were constructed to provide the necessary tuning waveform and to synchronize the signal processing at the output of the receivers with the particular scanning method being used. For the sake of clarity, two signal processing blocks are shown in Figure 4; however, only one has actually been constructed for testing in the developmental stages of the program.

2. R-F SECTION

The most important component in the microwave section of the DBFSR is the varactor-tuned Gunn diode microwave oscillator. This device produces approximately 100 mW of output power at a variable frequency from 8.5 to 9.5 GHz, depending on the bias voltage applied to the enclosed varactor diode. A thermostat controlled oven is used to provide a stable operating temperature for the components within the metal casing of the device.

Gunn effect diodes have many desirable features, including low noise, low bias voltage, wide bandwidth, and high reliability. The broadband negative resistance of the Gunn diode and the fact that its impedance tends to be less reactive than other microwave diodes are the reasons it is popular for use in varactor tuned circuits. Unfortunately, the high impedance of the varactor diode makes it susceptible to noise, so some care must be taken to shield the tuning input to the device. The Gunn oscillator (Greenray Industries, Inc. Model EPH-172-1) has a 470 picofarads capacitor shunting the input terminal to ground for reducing the effects of noise on the varactor.

The results of test performed on the Gunn oscillator are given in Table 1. The outpout power which the oscillator produces does not vary considerably over the specified bandwidth of 8.5 to 9.5 GHz. It is evident from the data that the tuning voltage and frequency do not exhibit a linear

Reference

5. Hilburn, J. L. and F. H. Prestwood. Principles of Frequency-Scanned Arrays, AFATL-TR-72-21, USAF Armament Laboratory, Eglin AFB, Florida. February 1972.

15

TABLE I

Experimental Test Results

for the Varactor Tuned Gunn Oscillator

Frequency GHz	Tuning Voltage(V)	Total Power Out (mW)
8.4	17.5	
8.5	18.2	106
8.6	19.0	106
8.65	19.3	
8.70	19.6	107
8.75	20.0	
8.80	20.5	110
8.85	21.0	
8.90	21.5	111
8.95	22.0	
9.0	22.6	115
9.05	23.4	
9.10	24.0	115
9.15	24.6	
9.20	25.4	112
9.25	26.6	
9.30	27.6	106
9.35	28.5	
9.40	29.9	101
9.45	31.8	
9.50	33.0	100
9.55	34.9	
9.60	37.4	96

dependence, an expected result in view of the fact that the capacitance of the varactor diode junction is exponentially related to the voltage across it. These data were useful in designing the circuits of the digital-to-analog (D/A) converter that generates the stairstep voltage needed for stepped scanning of the antenna arrays. These data were also needed to a lesser degree in the design of the ramp tuning voltage generator. When the linear ramp voltage is applied to the varactor diode, the resultant sweep of the array patterns across the target area is predictably non-linear - - a somewhat less than desirable method of operation.

An SMA coaxial connector feeds the output of the Gunn oscillator to a four port directional coupler (Figure 6). This coupler divides the r-f energy into two equal parts while maintaining a minimum of 15 dB of isolation between the output ports. A power divider splits the energy from the direct port of the directional coupler and provides local oscillator power to the three mixers. The other output from the directional coupler feeds a two-way power divider, which in turn feeds a two-way power divider that feeds power to the two transmitting antenna arrays. Waveguide isolators are used between the four antenna arrays and their respective feed lines, and coaxial-to-waveguide adapters are used for mating the coaxial power dividers to the waveguide components. Some reflections occur in the power allocation devices, but measurements have indicated that the power to the mixers is maintained above 2 mW, the minimum local oscillator power needed in order to obtain a 6 dB noise figure for the mixers (Reference 3).

3. I-F SECTION

The receivers of the DBSFR operate on the superheterodyne principle, wherein the received signal is mixed with a local oscillator signal of higher frequency (Reference 6). The received signal can be represented as an amplitude modulated signal with a large carrier term, which can be expressed as $[A + f(t)] \cos \omega_c t$; where $f(t)$ represents the modulating signal and A represents the carrier term. The local oscillator is a sinusoid of some higher frequency $\omega_c \pm \omega_i$. The mixer operation can be represented by:

$$[A + f(t)] \cos (\omega_c t) \; B \cos (\omega_c \pm \omega_i)t = \qquad (1)$$

$$\frac{1}{2} [A + f(t)] B \cos (2\omega_c + \omega_i)t + \frac{1}{2} [A + f(t)] B \cos \omega_i t$$

Reference
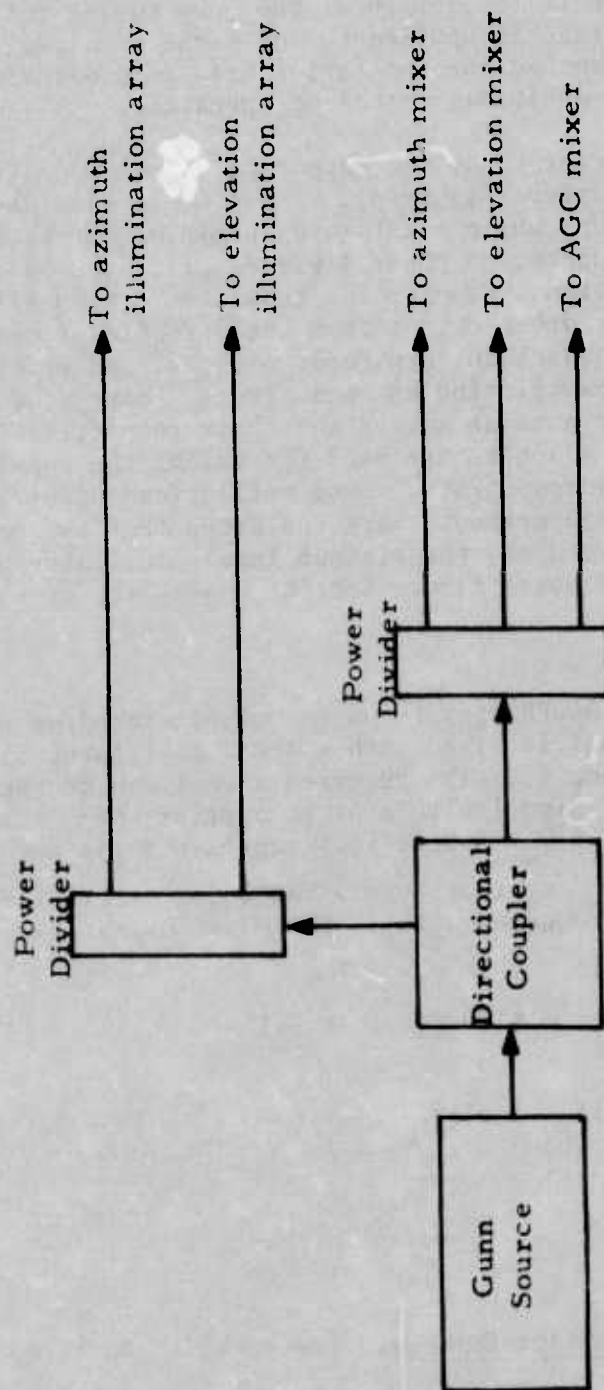6. Lathi, B. P. Communication Systems. New York: John Wiley & Sons, Inc., 1968.

17

Figure 6, Power Allocation Used in the Microwave Section of the DBFSR.

18

The first term on the right hand side of Equation 1 is beyond the i-f bandwidth and is filtered out, but the second term is at the center of the i-f passband (ω_i) and will be amplified. The amplified i-f signal is coupled to the detector. The detector in the DBFSR is a square law detector, and its output will be proportional to $[A + f(t)]^2$.

Note that if $\omega_i = 0$ (that is, if the incoming signal and the local oscillator signal are of the same frequency), then no i-f signal will be generated in the mixer. This property provides very good isolation between the transmitting and receiving sections of the DBFSR because the local oscillator signal is taken from the same source that generates the transmitting power. An i-f signal is generated only if the transmitted signal returns after a time span that is long enough for the tuning voltage waveform to change the frequency of the Gunn source. The time lapse necessary for the return signal to produce an i-f signal is dependent on the rate at which the local oscillator frequency is changed.

The preamplifiers which follow the mixers provide nominal gains of 25 dB from 30 to 180 MHz. Four transistor stages with series LC tuned circuits are used in these amplifiers. A postamplifier-detector module follows the preamplifier in each receiver, where six transistor stages, which are also LC series tuned, provide a gain of 50 dB. The first stage of this amplifier is provided with an external bias voltage by the automatic gain control circuits. The detector outputs are direct coupled to the video amplifiers, which can be adjusted to provide up to 60 dB of additional gain. A high speed FET operational amplifier (Intech Model A-130) is the primary component of the video amplifier modules. If the gain of the video stage is included, the overall gain of the receivers can be as high as 135 dB. This large gain is needed to compensate for the small amount of power used for illumination.

4. SCANNING AND TARGET DETECTION

Each of the four waveguide arrays used in the DBFSR is capable of scanning over about 10 degrees when the frequency is varied from 8.5 to 9.5 GHz (Reference 5). The arrays are designed such that they have a 3 degree half power (3 dB) beamwidth in the plane of the array and a 135 degree beamwidth in the transverse plane. The arrays are fastened to the system mounting board with the feed ends elevated such that the guide is at an angle of 8 degrees with the surface of the board (Figure 5). This angular mounting is necessary to align the center frequency (9.0 GHz) main beam angles with the perpindicular axis of the mounting board.

19

Stairstep Mode of Operation

The most promising method of scanning the arrays is the stepped method, which uses a stairstep tuning voltage to drive the Gunn source (Figure 7a). The voltage levels of this waveform are adjusted such that the Gunn oscillator output frequency is stepped from 8.7 to 9.5 GHz in 0.1 GHz increments during the sweep period. Each voltage level lasts for one clock period, except for the first and last voltage levels.

The voltage levels of the tuning waveform correspond to eight different angles for the main beams of the receiving arrays, thus the azimuth and elevation scan volumes can each be divided into eight 3 by 135 degree sectors. These sectors will overlap somewhat because a 100 MHz frequency step creates an angular displacement that is less than the 3 dB beamwidth of the arrays.

To understand the operation of the stepped mode, consider a transmitting array during some clock period when the Gunn source is at frequency f_1, and sector S_1 is being illuminated at the time by this array. Suppose a stationary target is in S_1 at a distance d from the system. The energy at frequency f_1 will take time t_p to traverse the distance to and from the target, where t_p is given by:

$$t_p = 2d/c \qquad (2)$$

Where:

t_p is the two way propagation time.

d is the distance to the target.

c is the speed of light.

Part of the reflected energy from the target will be coupled to the mixers by the receiving array, but because the local oscillator frequency is still at f_1, no i-f signal is generated. At the end of a clock period, the Gunn oscillator will be stepped to another frequency, $f_2 = f_1 + 100$ MHz, and the array beam will illuminate another sector of the scan volume, for example, S_2. However, the receiving array will continue to receive the reflection from the target due to the energy of frequency f_1 which is in transit to and from the target. This "in transit" energy
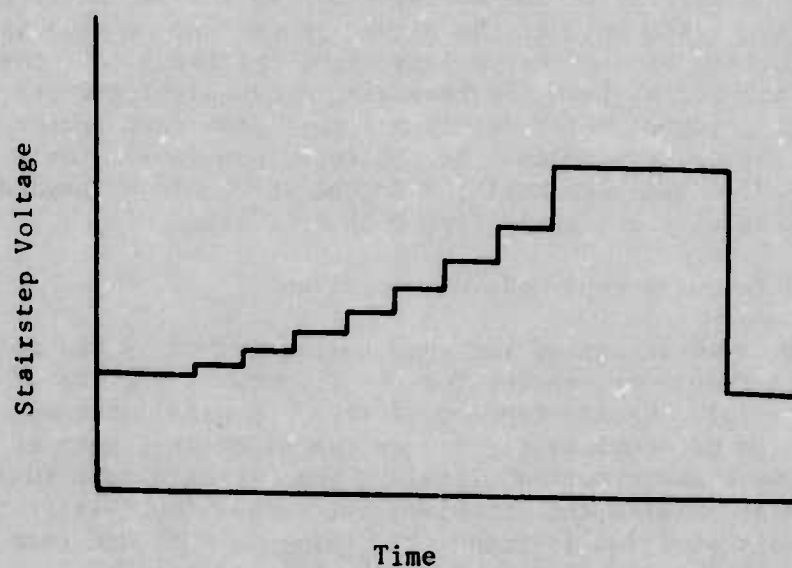
(a) Stairstep Mode of Operation.

Figure 7. Ideal VCO Tuning Voltage.

will endure for t_p seconds, and an i-f signal will be generated during this clock period due to the reflected signal of frequency f_1 mixing with the local oscillator signal. If the rise time associated with the frequency step from f_1 to f_2 is t_r, then the approximate duration of the i-f signal will be $t_p - t_r$.

Since the scanning operation is being carried out in both an azimuth and elevation plane, it is possible to obtain the target location by noting the particular period during which an i-f signal is generated in each receiver. The role of the signal processing section is to divide the detected output of a receiver into eight intervals that correspond to the eight sectors from which the receiving array might receive reflected energy, and it integrates the detected signal from each sector over hundreds of sweeps of the antenna beams. As mentioned previously, only one signal processing section has been built; a second one would be needed for simulaneous processing of the signals from both receivers.

Ramp (Continuous Sweep) Mode of Operation

The main advantage of the ramp tuning method is the absence of rapid jumps in frequency, except for the flyback at the end of a sweep period (Figure 7b). Rapid stepping of the Gunn oscillator was found to cause generation of spurious signals in the mixer that were of sufficient magnitude to mask any received signals. The use of a ramp tuning voltage only slightly alleviated this problem, but it was found later that the spurious signals were low in frequency, below 30 MHz, and that they could be attenuated by further filtering in the i-f amplifiers.

When the DBFSR is operating in the continuous sweep mode, the Gunn oscillator is tuned by the periodic linear ramp or sawtooth voltage. The frequency of the sawtooth voltage is typically about 22.2 kHz. If the tuning characteristic of the Gunn source is assumed to be linear, then the frequency of the oscillator output would increase linearly with the ramp voltage. The frequency modulated output of the source could be analayzed further by utilizing Fourier series techniques and multitone frequency modulation concepts. Fortunately, for the case under consideration, a more simplistic approach is possible because the deviation ratio (the ratio of total instantaneous frequency deviation to the maximum rate of instantaneous frequency deviation) of the Gunn r.f. output is quite large.

A typical worst-case (high sweep rate) deviation ratio is given by

$$(9.5 - 8.5) \ 10^9/50 \times 10^3 = 2 \times 10^4$$

22
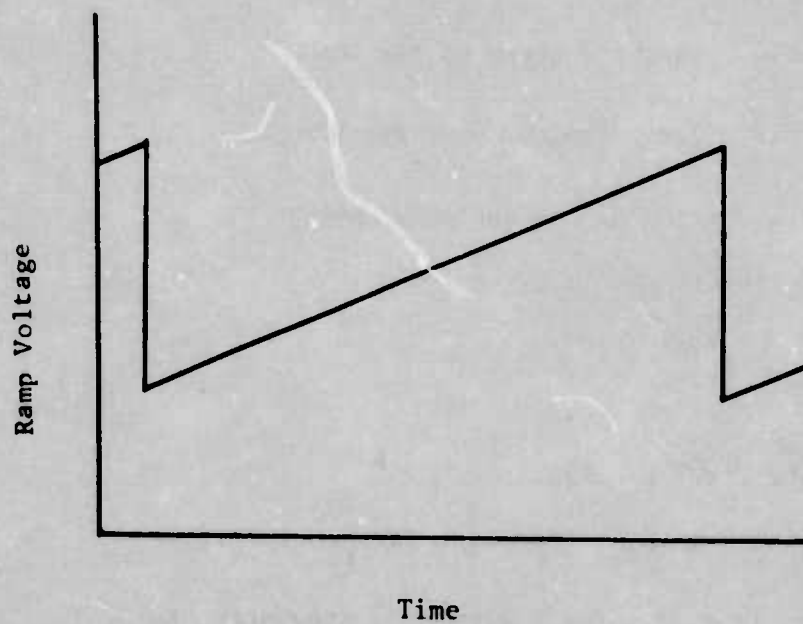
(b) Ramp Mode of Operation.

Figure 7. Ideal VCO Tuning Voltage.

23

Because of this very high ratio, the output of the Gunn voltage controlled oscillator (VCO) may be thought of as a sinusoid of slowly varying frequency (Reference 7).

The rate of frequency change, $\Delta f/\Delta t$, is given by

$$\Delta f/\Delta t = (f_2 - f_1)/T_s \qquad (3)$$

Where:

f_1 is the lowest frequency of the VCO.

f_2 is the highest frequency of the VCO.

T_s is the period of the sweep frequency.

The distance to the target is given by

$$d = ct_p/2 \qquad (4)$$

Where:

c is the speed of light.

t_p is the two way propagation time to target.

The propagation time, t_p, for a given i-f frequency, f_{i-f}, is

$$t_p = f_{i-f}/\left(\Delta f/\Delta t\right) \qquad (5)$$

For a 50 kHz sweep frequency (from Equation 3):

$$\frac{\Delta f}{\Delta t} = \frac{1 \times 10^9 \text{ Hz}}{0.2 \times 10^4 \text{S}} = 5 \times 10^{13} \text{ Hz}/ \qquad (6)$$

Reference
7. Carlson, A. Bruce. Communications Systems: An Introduction to Signals and Noise in Electrical Communications. New York: McGraw Hill Book Co., Inc., 1968.

24

If a sharp cutoff at 50 MHz is assumed for the i-f amplifier, then a minimum target distance can be calculated. The minimum time for a 50 MHz i-f frequency (Equation 5), is

$$t_{min} = t_p = 50 \text{ MHz}/5 \times 10^{13} \text{ Hz}/ = 1.0 \text{ } \mu s \tag{7}$$

Thus, the minimum distance to the target would be (from Equation 4):

$$d_m = ct_{min}/2 = 150 \text{ meters} \tag{8}$$

5. DIGITAL-TO-ANALOG (D/A) CONVERTER FOR STAIRSTEP MODE

The digital-to-analog (D/A) converter produces the stairstep waveform used as a tuning voltage in the stepped mode. The original D/A converter used with the system suffered from poor rise times of about 4 microseconds for the voltage steps it produced, as well as from a very poor fall time (flyback time) at the end of the sweep period (Reference 3). For these reasons, a new D/A converter was needed. Since the problem in the original D/A converter was with the slow switching network and not with the logic used to drive the switches, the original logic network was retained to drive a new switching network. This logic network will hereafter be referred to as the D/A logic network, and the network which generates the stairstep waveform using the pulses of the D/A logic will be referred to as the D/A converter.

In the D/A logic network, the clock pulses are used to generate a sequence of 12 negative output pulses (Figure 8). A divide-by-twelve counter (S8288A) produces a four bit binary-coded-decimal (BCD) from the clock pulses, and this is fed directly to one binary-to-octal decoder (S8250a), which generates a one-of-eight output. These are the first eight outputs in the one-of-twelve sequence. The remaining four outputs are generated by another octal decoder that has the fourth digit (2^4) from the counter inverted at its enable input, thus keeping this decoder dormant until the binary number 1000 appears at the output of the counter. This count disables the first decoder and enables the second, allowing it to continue the sequence. After 12 counts, the counter resets to binary 0000, and a negative pulse appears at the Number 1 output as the sequence begins again. Each of the 12 outputs remains low for the duration of the clock pulse for that count.

The sequential output pulses from the D/A logic network were originally used to generate 12 voltage levels in the stairstep tuning voltage waveform. The new D/A converter, however, was designed to produce a stairstep voltage with nine voltage levels because this was adequate for full utilization of the eight available channels of signal processing. Since the initial clock period (and the first voltage level) after flyback is not useful receiver
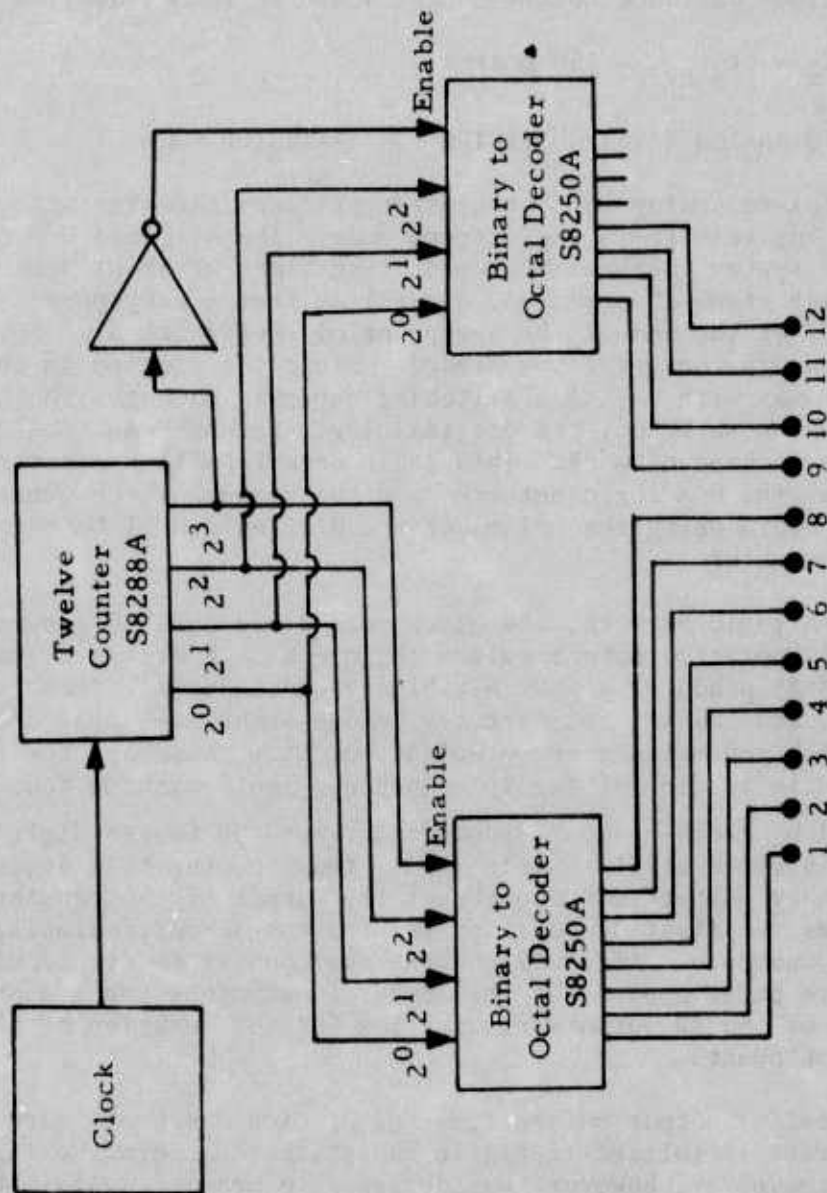
Figure 8. Digital to Analog Logic Section. (This circuitry produces twelve sequential negative pulses which are used in generating the stairstep tuning voltage waveform.

time, nine voltage levels are necessary for eight meaningful channels in
the signal processing section. During the first period, the transmitting
array is illuminating the sector of the scan volume that will correspond
to the first channel of signal processing during the next clock period.

As shown in Figure 9, four integrated circuits are used in the converter.
Each is an SN7476 dual master-slave J-K flip-flop: this provides eight
flip-flops, one for each transistor switch. The $\overline{Q}$ output of each flip-flop
holds the transistor (to which it is connected) in saturation until the
proper clock interval. The asynchronous inputs of the flip-flop are driven
by the Number 2 through Number 9 outputs from the D/A logic network (Figure
8), thus triggering the flip-flops and turning on the transistor switches
in sequence. The asynchronous inputs were used to avoid clocking the flip-
flops. Diodes couple the voltage on each resistive divider to a common
output line that drives the base of the output transistor. The emitter
follower configuration of this transistor provides a high input impedance
and a low output impedance. Low source impedance is important since the
tuning voltage terminal of the Gunn oscillator appears as a capacitive load
for this network. Figure 10 shows a partial schematic of the D/A converter,
and Table 2 gives the resistor values used in each transistor stage.

Trim potentiometers were used in the upper portion of each of the resistive
divider sections to allow precise adjustment of the voltage levels. The
tuning voltage versus frequency data (Table 1) were used in designing the
divider networks. When the Gunn oscillator is driven by the stairstep voltage,
the microwave output has nine frequency components corresponding to the nine
voltage levels. These components were tuned by using a microwave frequency
meter and a power meter connected to the output of the oscillator. The trim
potentiometers of the divider networks were adjusted until the power meter
indicated output frequencies at 0.1 GHz increments from 8.7 to 9.5 GHz.
Figure 11 shows an oscillogram of the output of the D/A converter.

6. SYSTEM CLOCK

The improved rise time of the D/A converter made it possible to use
faster clock rates than was originally designed into the system. A new
clock was constructed using a Signetics NE555 timer integrated circuit.
This device was chosen because it could be used in a simple astable circuit
configuration which offered variable clock rate capability. It also provides
excellent frequency stability, and it is compatible with TTL logic. Figure
12 shows the circuit configuration in which the NE555 is operated and the
block diagram of the functional parts of the circuit. The trigger (pin 2)
and threshold (pin 6) are shorted together for self triggering. When the
output of the NE555 is low, the capacitor C is charging through resistors
R_A and R_B towards the supply voltage, V_{cc}. When the capacitor voltage
equals 2/3 V_{cc}, the comparator triggers the internal flip-flop, causing
the output to go high and the discharge cycle to begin. The discharge
transistor drains the capacitor through the resistance of R_B, until the
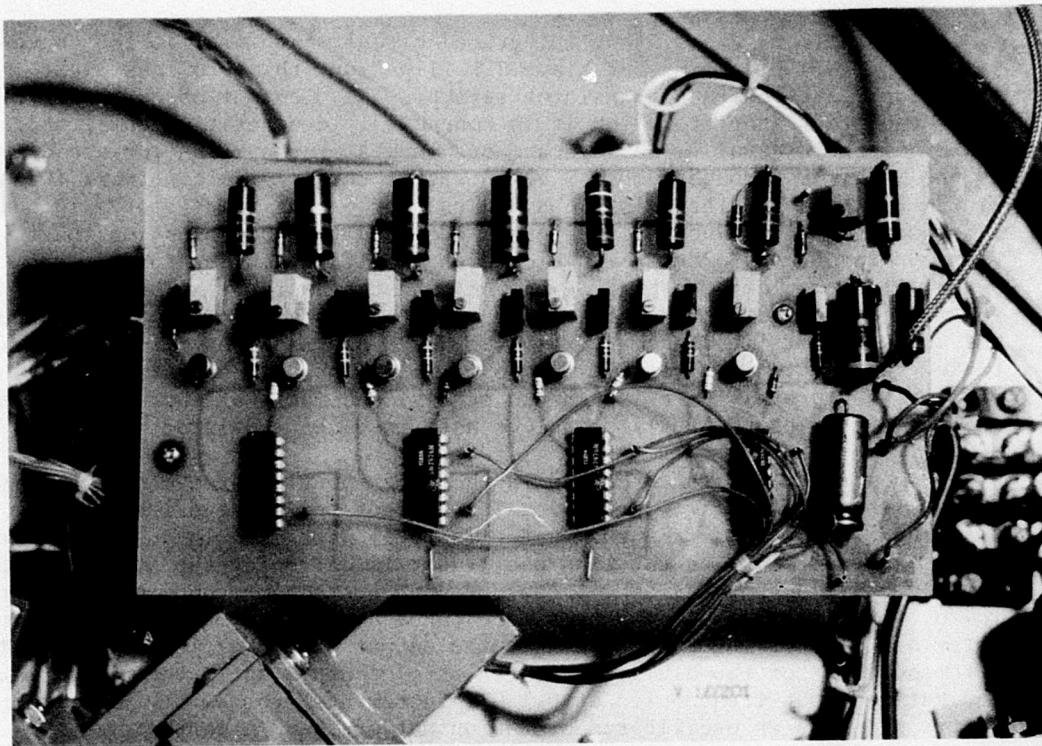
27

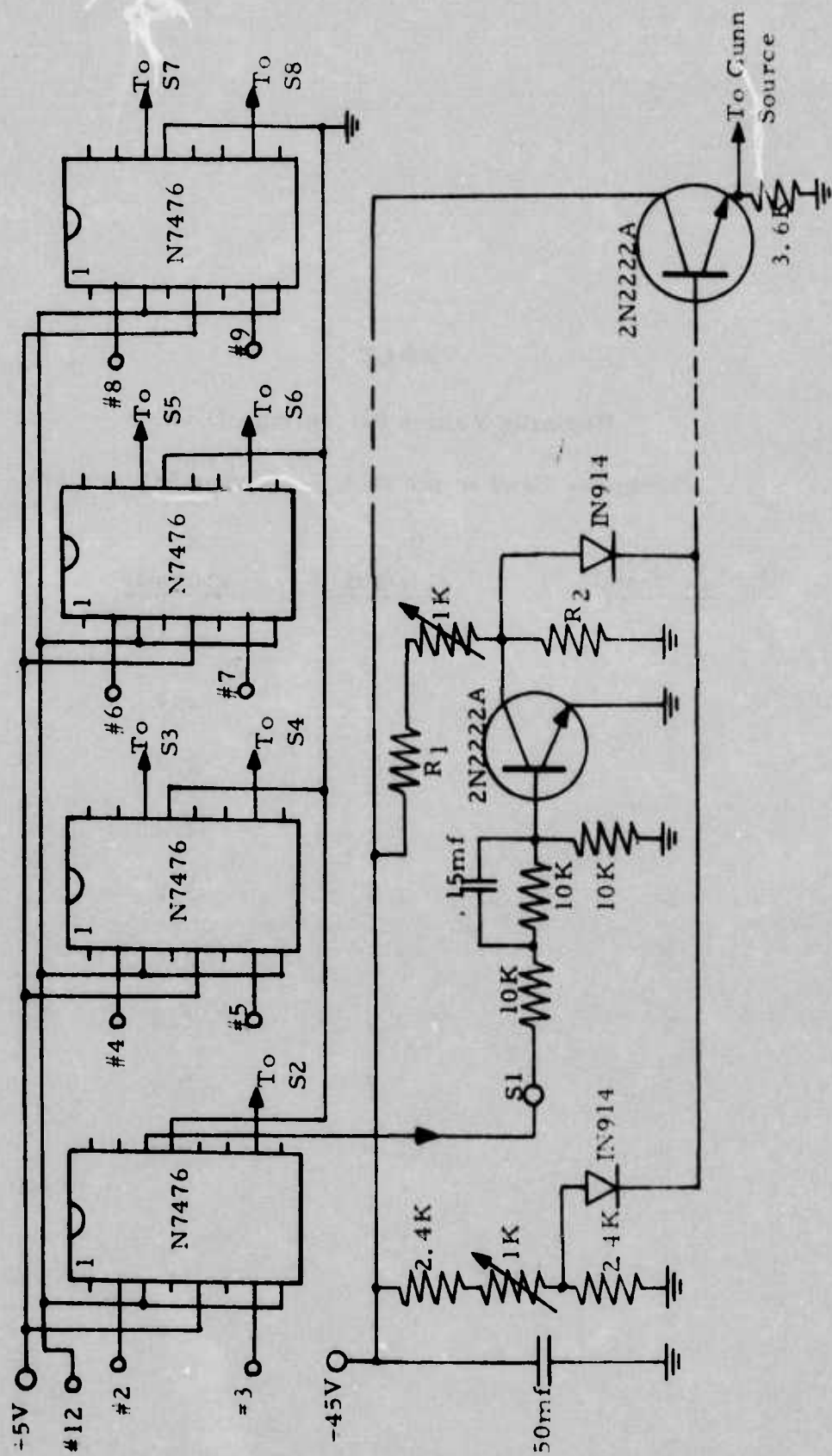Figure 9. Top View of Circuit Board for D/A Converter.

Figure 10. Partial Schematic for the D/A Converter. (Values of R_1 and R_2 for the eight transistor switches (S1-S8) are given in Table 2.)

29

TABLE 2

Resistor Values for Voltage Divider

Networks Used in the D/A Converter (Figure 18)

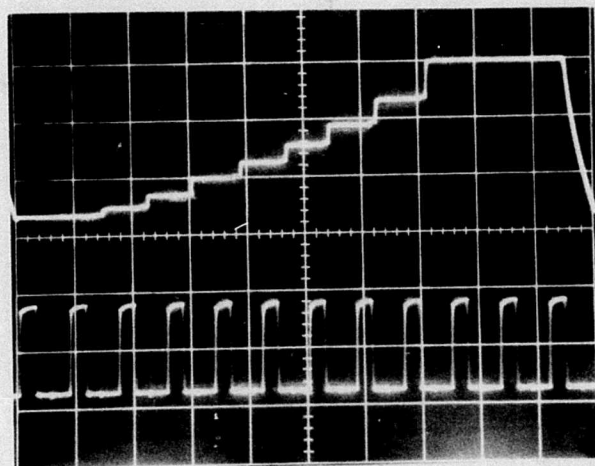| Voltage Level	R_1 (KILOHMS)	R_2 (KILOHMS)
1	2.4	2.4
2	5.1	2.4
3	2.0	2.4
4	2.0	2.7
5	2.0	3.0
6	2.0	3.6
7	2.0	4.3
8	2.2	5.6
9	2.0	6.8

Figure 11. D/A Converter Output (Upper Trace;
            Vertical Scale = 5V/Div., Horizontal
            Scale = 5µs/Div.) and the System Clock
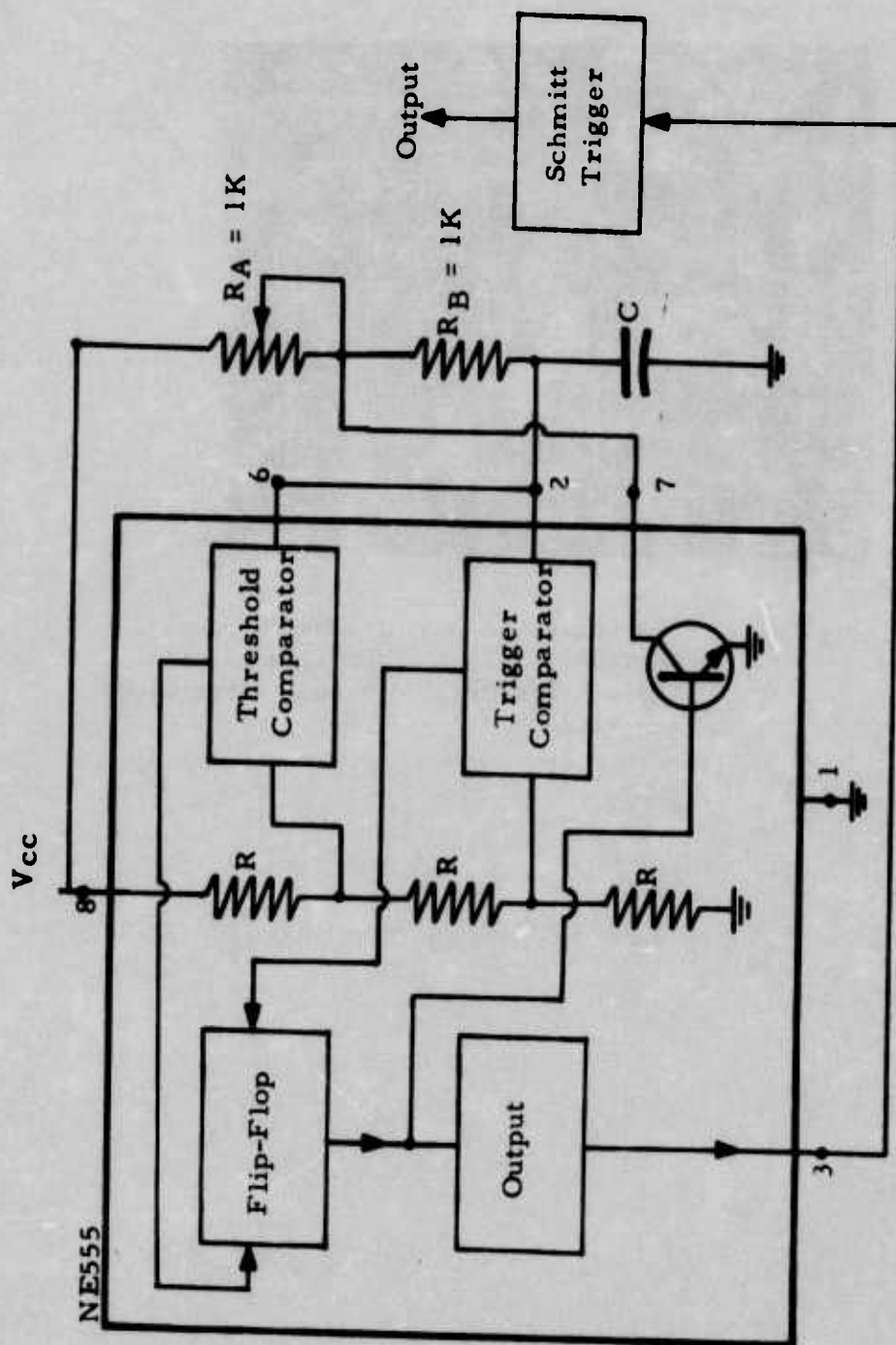   (Vertical Scale = 2V/Div.).

Figure 12. Linear Integrated Circuit as used in the Clock Circuitry of the DBFSR.

voltage on the capacitor falls to $1/3 \, V_{cc}$. Then the trigger comparator triggers the flip-flop again, causing the output to go low and ending the discharge period. The use of voltage ratios set by the internal resistors makes the operation of the circuit essentially independent of the supply voltage. The output of the NE555 provides ample current to drive the TTL Schmitt trigger which is used to buffer the output of the oscillator.

The ramp generating circuitry used for the DBFSR required that oscillations of the clock be synchronized to those of another oscillator. This was not ideal, but it proved to be necessary. The clock oscillator was held in synchronism with a ramp function generator (NE566) by pulsing the trigger pin with a negative voltage of sufficient magnitude to overrride the normal discharge cycle and to fire the trigger comparator.

7. SIGNAL PROCESSING SECTION

The output of the video amplifier must be referenced in some manner that separates the signal recieved during the different portions of the sweep period. If this is done, it is possible to determine the relative position of a reflective target by the occurrence of its return signal within the sweep period. The signal processing section accomplishes this task.

The block diagram for the logic and processing section, as used when the system is in the stepped mode, is shown in Figure 13. The necessary switching function is provided by two AM3705 eight channel analog multiplexers. The AM3705 uses MOSFET p-channel devices operating in the enhancement mode for switches. Since these MOSFET switches are bilateral devices, the AM3705 can be used in either a demultiplexer or a multiplexer fashion.

The multiplexer integrated circuit incorporates an octal decoder that determines which of the eight switches are to be opened according to the state of the three line BCD input. The BCD is provided by an N7490 counter (Figures 14 and 15). The multiplexer also has an enable pin which opens all of the switches when the pin is in the low state.

In the processing circuitry, the first AM3705 is used to switch the output of the video amplifier to the inputs of eight integrators. The BCD input to the multiplexers is synchronized with the clock, and in the stepped mode, a different integrator is switched in for every step in frequency of the Gunn sources. This first AM3705 is operating as a demultiplexer. The second AM3705 simultaneously multiplexes the integrator outputs to one output line in the same sequence as the inputs are switched.
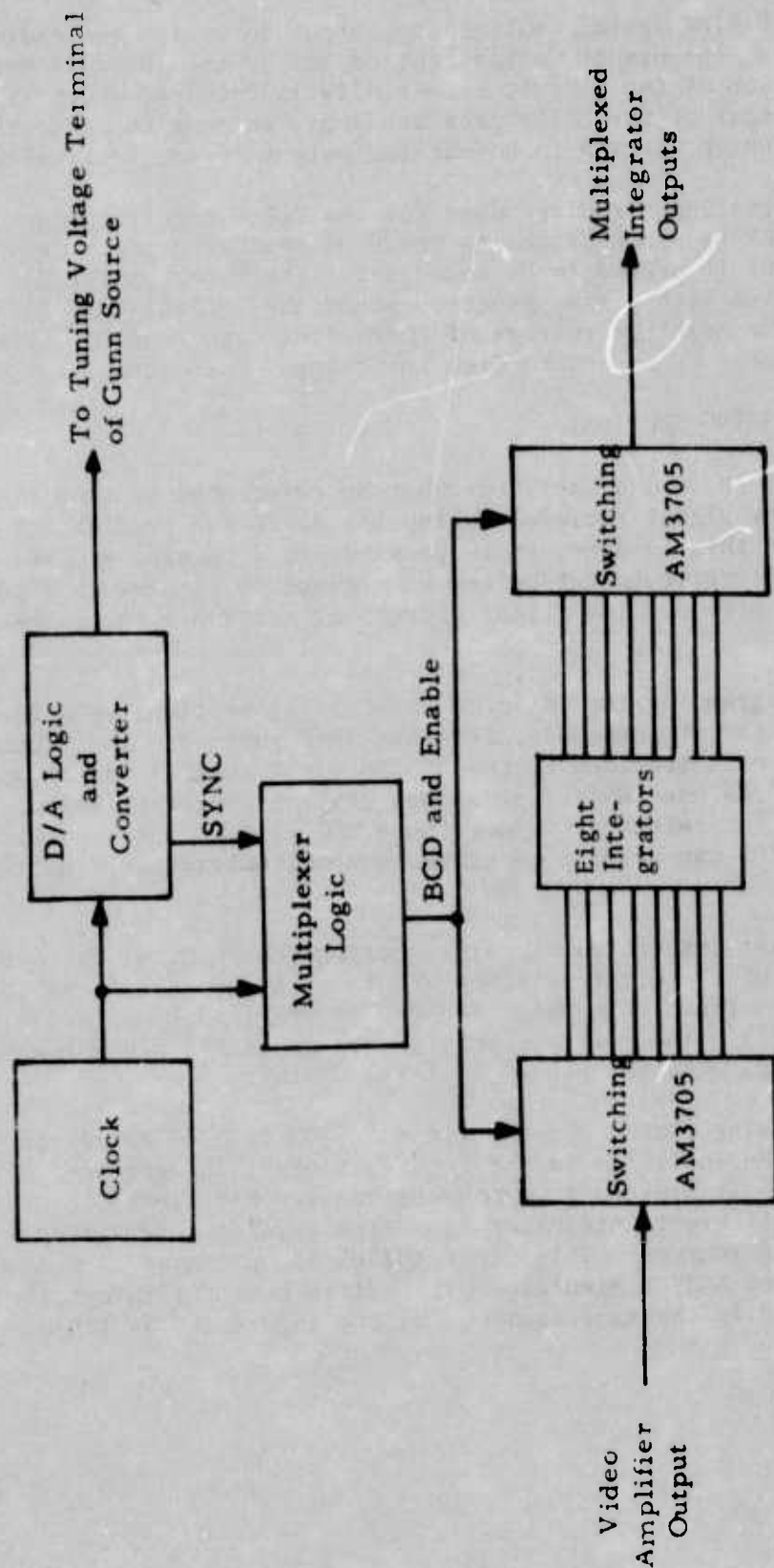
Figure 13. Logic and Processing Circuits used when the DBFSR is Operated in the Stepped Mode.
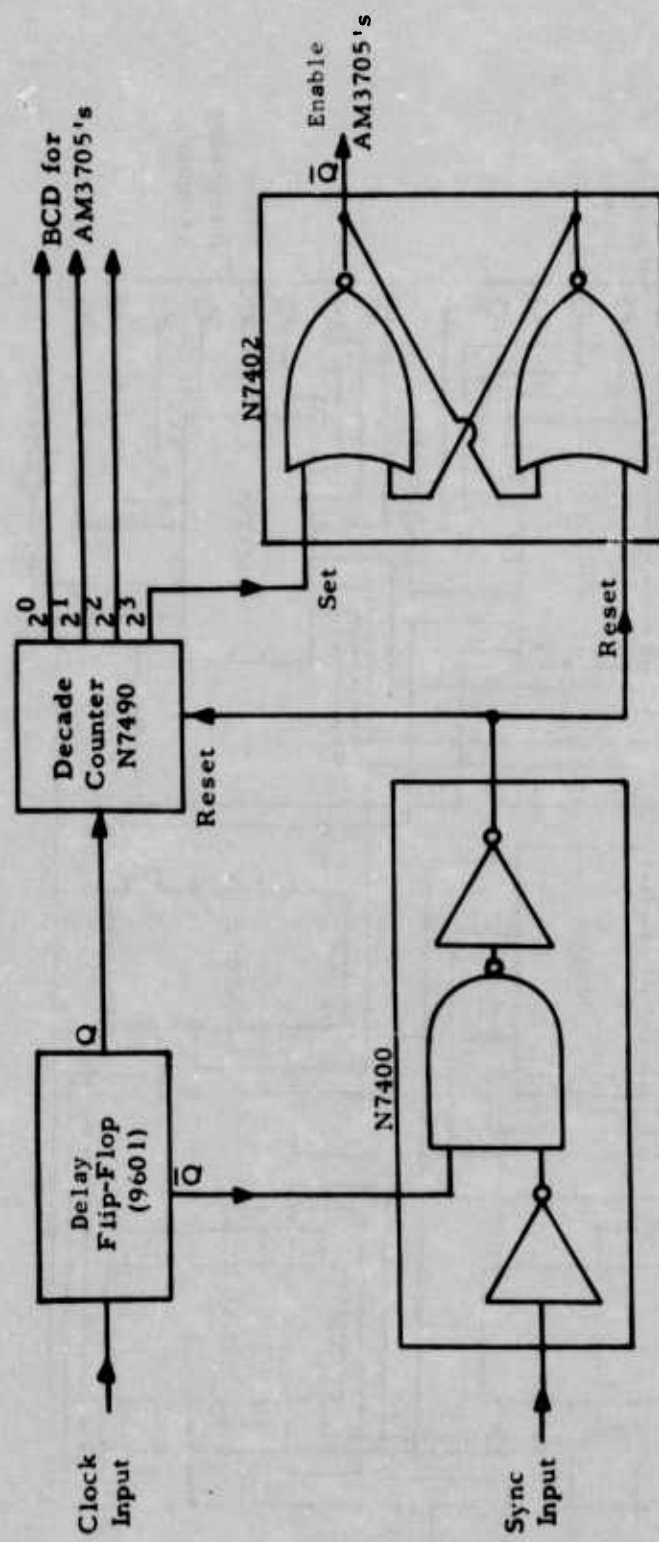
34

Figure 14. Circuits Providing BCD and Enable Inputs to the AM3705 Multiplexers.
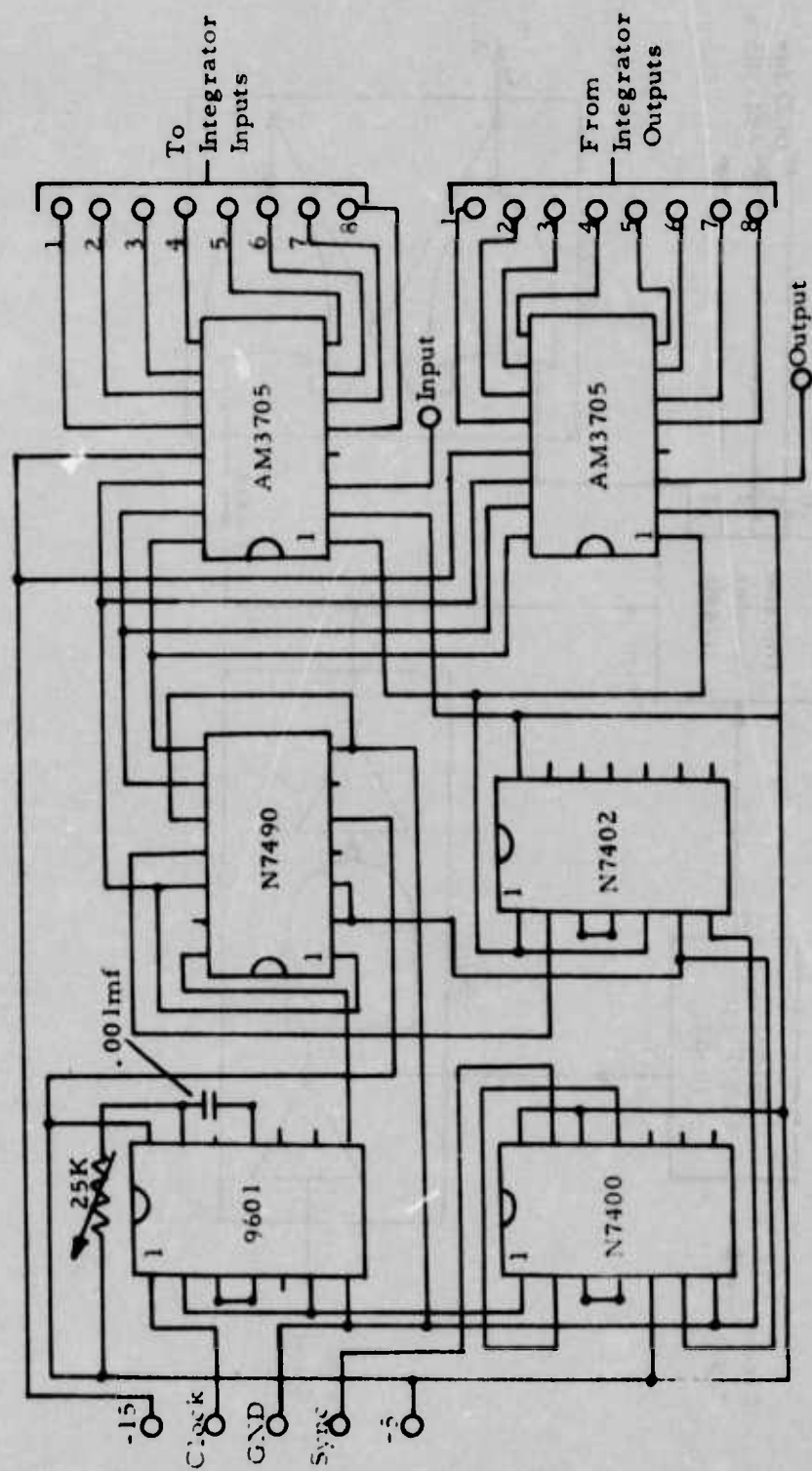
Figure 15. Multiplexing Circuitry and Associated Logic.

When the processing circuitry was constructed, only the AM3705 integrated circuits were available, and this limited the capacity of the circuitry to eight channels. The D/A logic resets every twelfth clock pulse, so the multiplexers must be disabled for a portion of the sweep period. The multiplexer logic circuits provide the necessary BCD and enable pulses.

The logic circuitry for the multiplexers is shown in Figure 14. An N7490 high speed decade counter provides the BCD input for the multiplexer. This TTL integrated circuit is comprised of four master-slave flip-flops, which are connected internally as a divide-by-two and divide-by-five counter. A four fit BCD count is obtained by connecting the divide-by-two output to the divide-by-five input. The first three digits (2^0, 2^1, 2^2) of the BCD output form the input to the multiplexers, and the fourth (2^3) digit is used to "set" an R-S (Reset-Set) flip-flop which is constructed from two NOR gates of an N7402 TTL integrated circuit. When the 2^4 digit of the N7490 output goes to the high state, the multiplexers are disabled because the $\overline{Q}$ output of the R-S flip-flop then goes to the low state, and they remain disabled until a sync pulse from the D/A converter is gated through to "reset" the flip-flop, causing the $\overline{Q}$ output to return to the high state and thus enable the multiplexers. The same sync pulse also resets the N7490 counter. This sync pulse, which is taken from the Number 2 output of the D/A logic (Figure 8), starts the processing of the input signal.

The transistor switching circuitry of the D/A converter is slower than that of the multiplexers, and it is necessary to delay slightly the clock pulses which drive the multiplexer logic. This is done by a monostable flip-flop triggering on the negative edge of the clock pulses (Figure 14). A variable resistor is used in the timing circuit of the monostable device to vary the amount of delay and thus allow precise synchronization of the steps in the tuning voltage with the opening of the multiplexer switches. The inverted ($\overline{Q}$) output of the monostable flip-flop is used to gate the sync pulse from the D/A logic such that it is delayed by the same amount as the clock input. A timing diagram for the multiplexer logic is shown in Figure 16.

This switching and processing circuitry could be easily expanded to a 12 channel circuit by the addition of two more AM3705 multiplexers and another N7490 counter. Additional integrators would also be needed, of course. The expanded circuit would activate the additional counter and the multiplexers when the output of the first counter reached the binary 1000 state. These components would then continue the switching of the video amplifier output to the additional integrators.
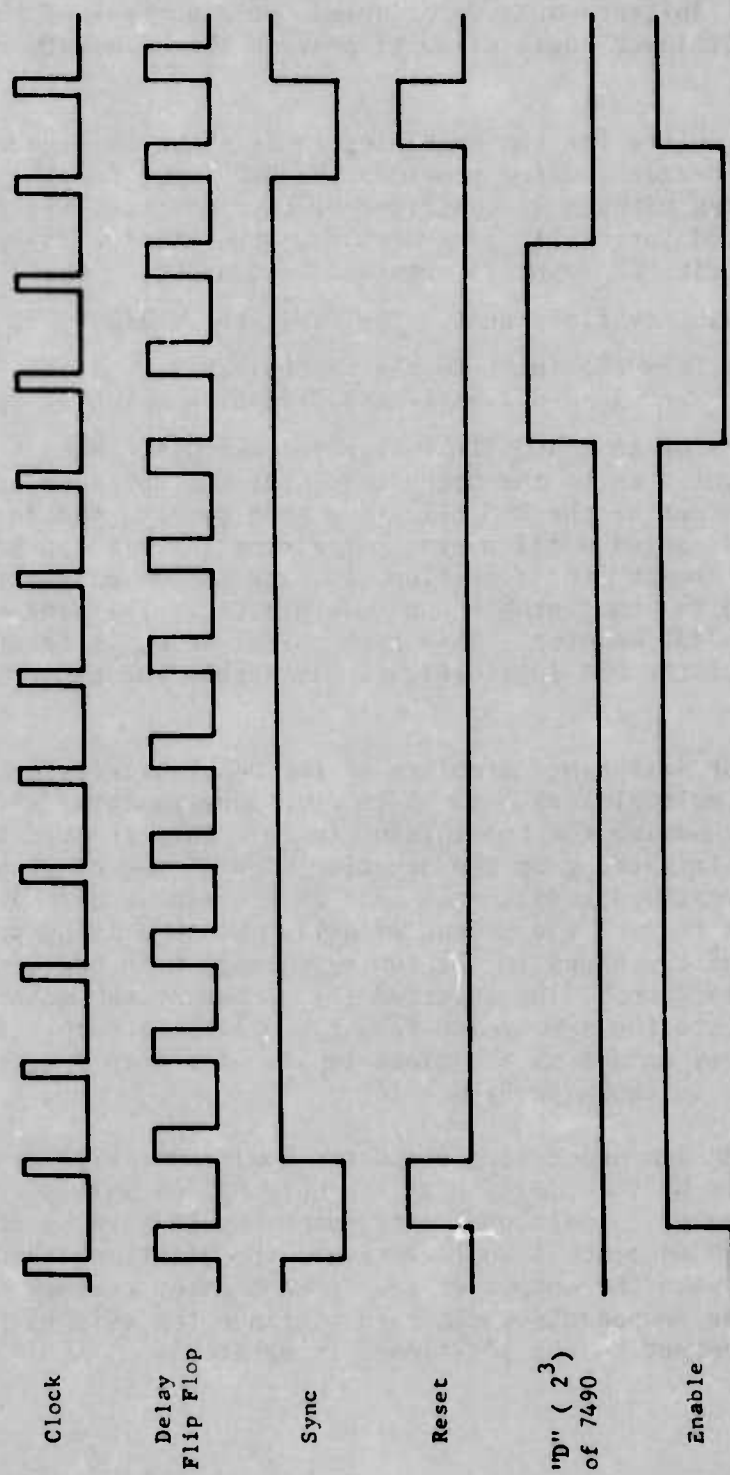
Figure 16. Timing Diagram for Multiplexer Logic.

38

When a transmitting array beam is being frequency stepped, the different sectors of its scan volume are in effect being pulsed with microwave energy for one clock period during each complete sweep of the array beam. The corresponding received energy from each sector of the scan volume is combined over many sweeps by the eight separate integrators. The circuitry of the integrators (Figure 17) uses an uA741 linear operational amplifier with a resistor and a capacitor in parallel as feedback elements. The d.c. voltage level of the non-inverting input can be varied to accommodate the d.c. level that appears at the output of the video amplifier. The integrators are operated from a $\pm$ 5 volt power supply so that the output does not exceed the maximum voltage allowed for the AM3705 multiplexers.

If the uA741 is approximated as an ideal operational amplifier with infinite gain and input impedance, it can be shown that the transfer function of the circuit in Figure 17 is given by: (Reference 11)

$$H(s) = \frac{-Z_i(s)}{Z_f(s)} = \frac{-1/R_1 C}{s + 1/R_2 C} \tag{9}$$

Where:

$H(s)$ is the transfer function.

$Z_f(s)$ is the feedback impedance.

$Z_i(s)$ is the input impedance.

The inverting gain of this circuit is given by R_2/R_1, and the time constant is given by $1/R_2 C$. Using the component values of Figure 17, the gain of the circuit is a maximum of 50, and the time constant is 0.1 second. For a typical clock rate of about 240 Hz, the sweep rate is one-twelfth of that, or 20 Hz. Thus, about 2000 sweeps are performed within the time constant of the integrator circuits.

8. RAMP-MODE CIRCUITRY

The continuous sweep mode requires a ramp tuning voltage for the Gunn source. A circuit for ramp voltage generation can be readily fashioned by using the NE566 linear integrated circuit. Normally, the output of this function generator is a triangle wave and a square wave, but with external modifications, a ramp (or sawtooth) waveform and a pulse waveform can be generated. A functional block diagram of the integrated circuit is given in Figure 18, along with the output modifying circuit. The normal triangle wave output is obtained by using constant current sources to charge and discharge the external capacitor C_1 through the
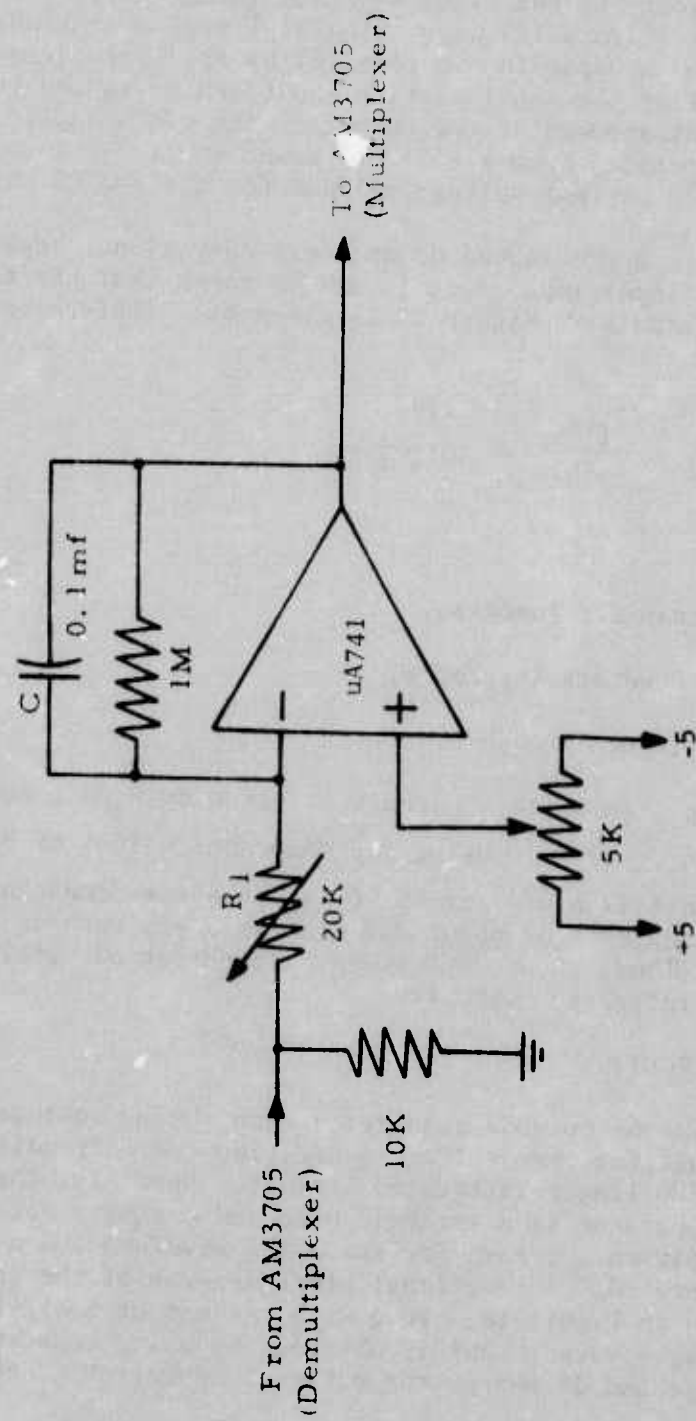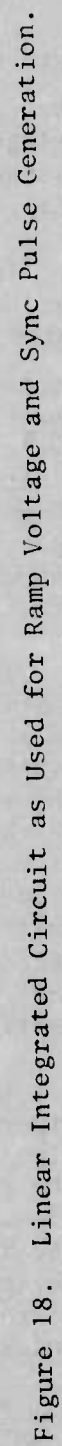
Figure 17. Integrator Used for Processing the Output of the Video Amplifier.

Figure 18. Linear Integrated Circuit as Used for Ramp Voltage and Sync Pulse Generation.

external variable resistor R_1. The voltage across the capacitor is buffered through an output stage to produce the triangle wave output. A Schmitt trigger senses the voltage level on the capacitor and controls the charge-discharge cycle. The Schmitt trigger output is also sent to a buffer amplifier to produce a square wave output.

In the modified circuit, the normal discharge cycle is aborted because as the square wave output goes to the high state, the transistor that is shunting the timing capacitor, C_1, turns on and rapidly drains off the stored charge. The lower threshold voltage for the Schmitt trigger is quickly reached, and its output falls to the low state, starting the charge cycle again. The triangle wave is now shortened to a positive ramp with a short fall time, while the square wave output now produces a train of short pulses. A Zener diode is used in the base circuit of the discharge transistor to block a positive d. c. voltage that is always present at the output terminals of the NE566 generator. The Zener was chosen such that its reverse breakdown voltage is greater than this d. c. voltage.

The pulses which appear at point C are buffered through a transistor and used to trigger a monostable flip-flop. The inverted ($\overline{Q}$) output of this flip-flop is used to trigger the clock oscillator (NE555) and thus synchronize the clock to the NE566 generator. The normal (Q) output of the monostable device is used to reset a gating network which is described in the next paragraphs. The ramp voltage output of the function generator is amplified to the proper peak-to-peak voltage swing, shifted to the proper d. c. level, and then buffered through a transistor in an emitter follower configuration to drive the tuning voltage terminal of the Gunn source. The schematic diagram for the circuits used in generating the ramp tuning voltage is shown in Figure 19, and the schematic for the amplifier and driver transistor is shown in Figure 20.

The gating network used in the continuous sweep mode is shown in Figure 21. The function of this network is to delay the start of the signal processing operation by two clock periods after the fall time of the ramp tuning voltage. This interval is provided to allow the transient signals that appear in the i-f signal after the flyback period to subside. The delay is accomplished by gating out the first two clock pulses at the beginning of the sweep period and using this gated clock to drive the multiplexer logic network. The gating network also provides the proper sync pulse for the multiplexer logic.

The gated clock signal is obtained by using an N7490 counter to generate a BCD count and to gate out the clock pulses until the binary count of 0010 appears. This delays the start of signal processing until the third clock period after the start of a sweep period. The opening of the gating network triggers a monostable flip-flop that provides a sync pulse for the multiplexer logic. The schematic for the gating network is shown in Figure 22.
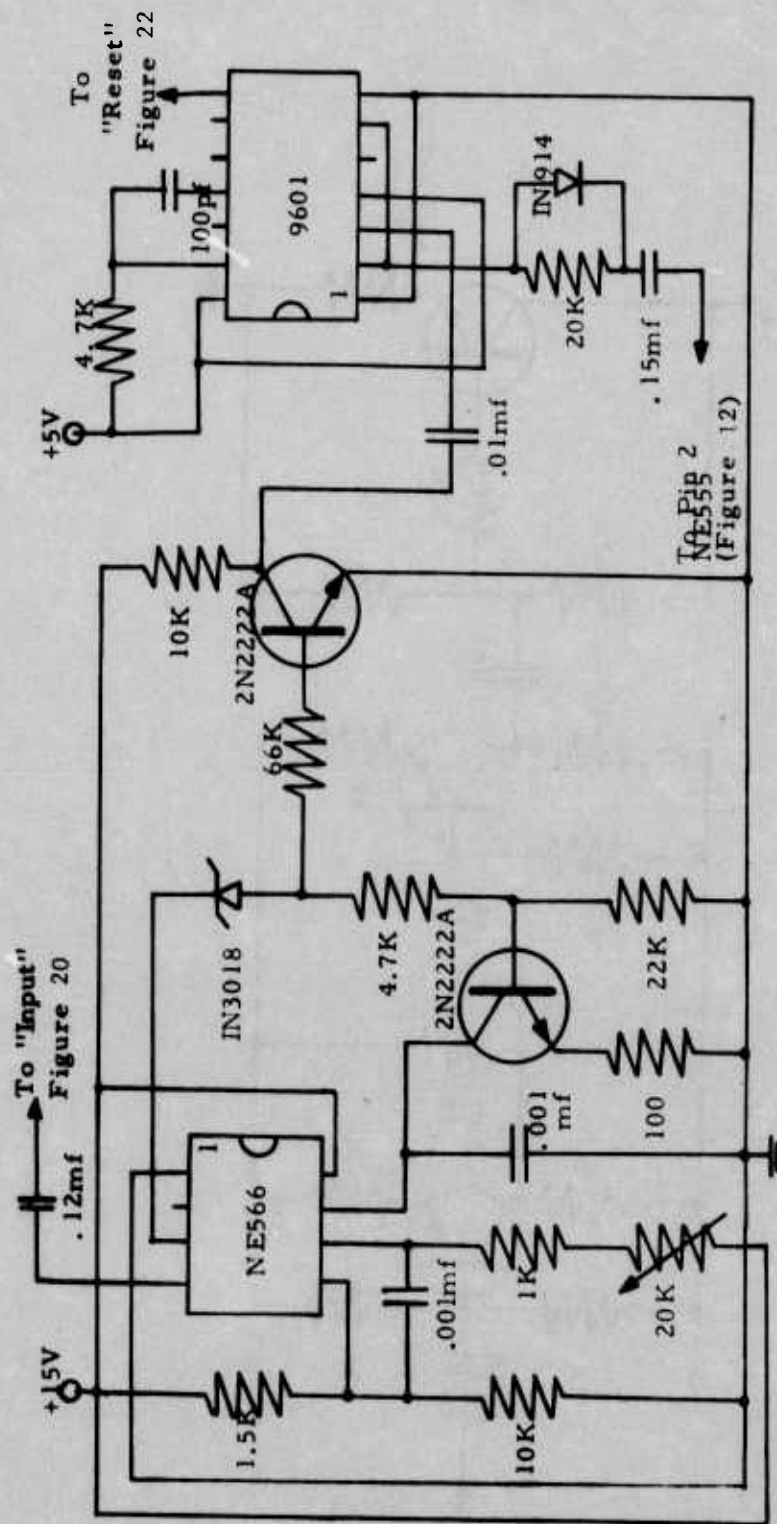
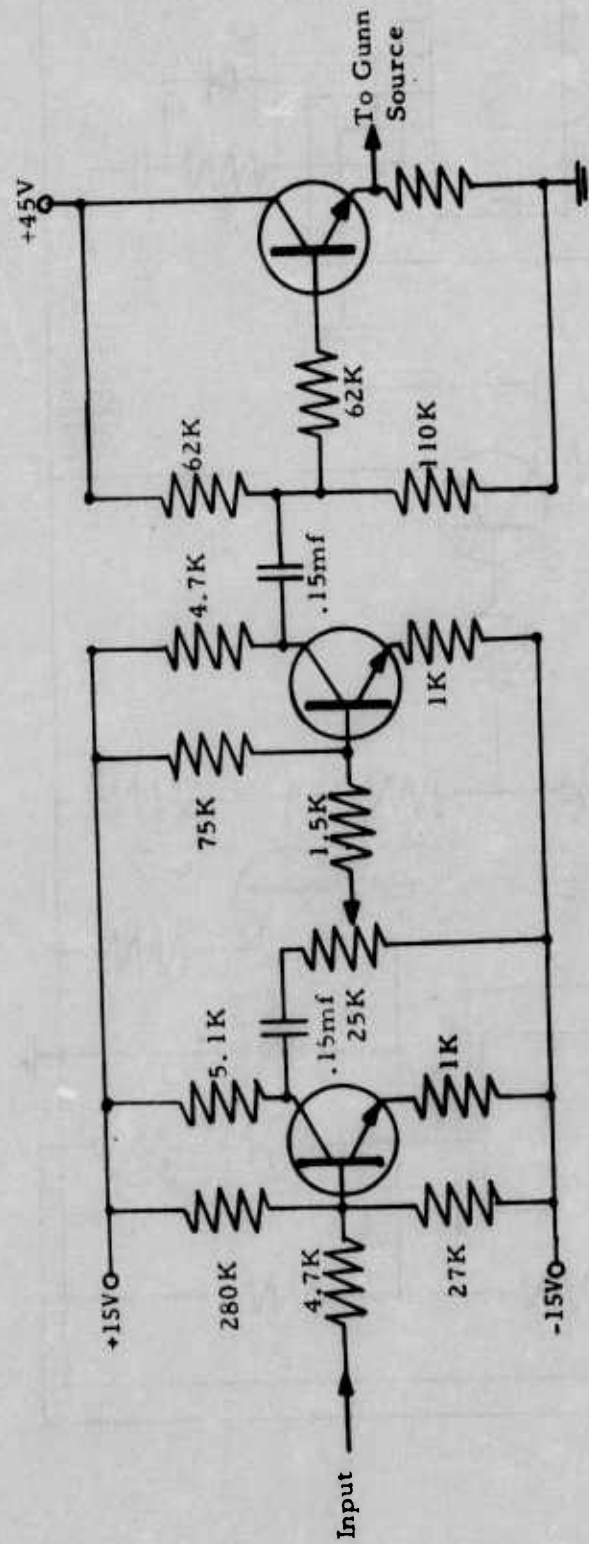Figure 19. Ramp Voltage Generator and Associated Sync Network.

Figure 20. Ramp Voltage Amplifier and Output Stage which Drives the Tuning Voltage Terminal of the Gunn Source. (All transistors are 2N2222A.)
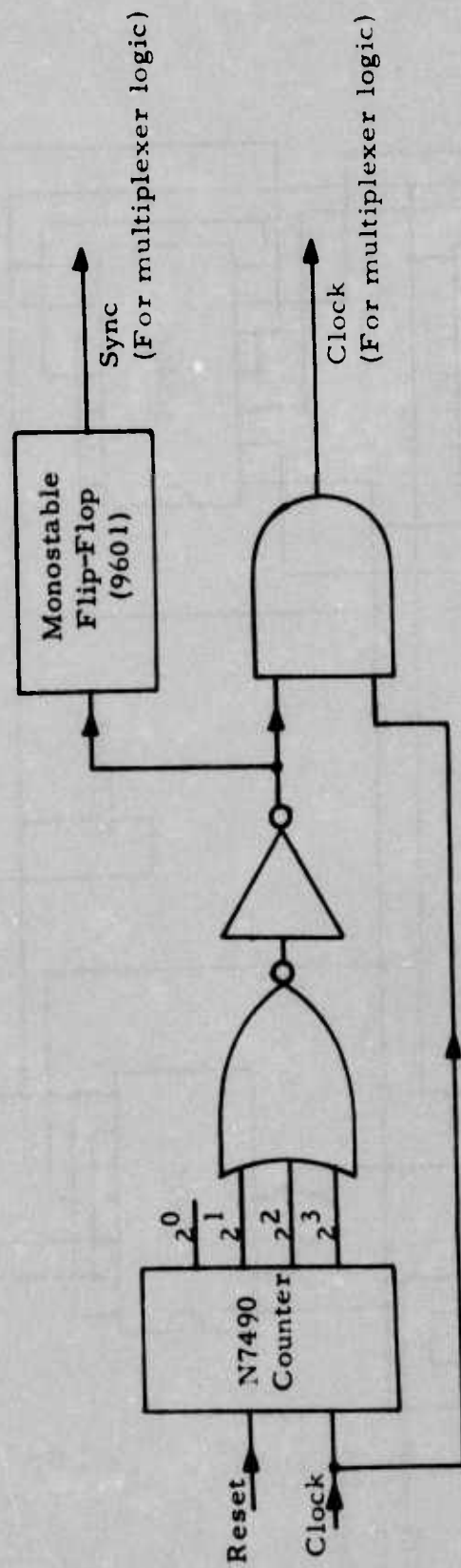
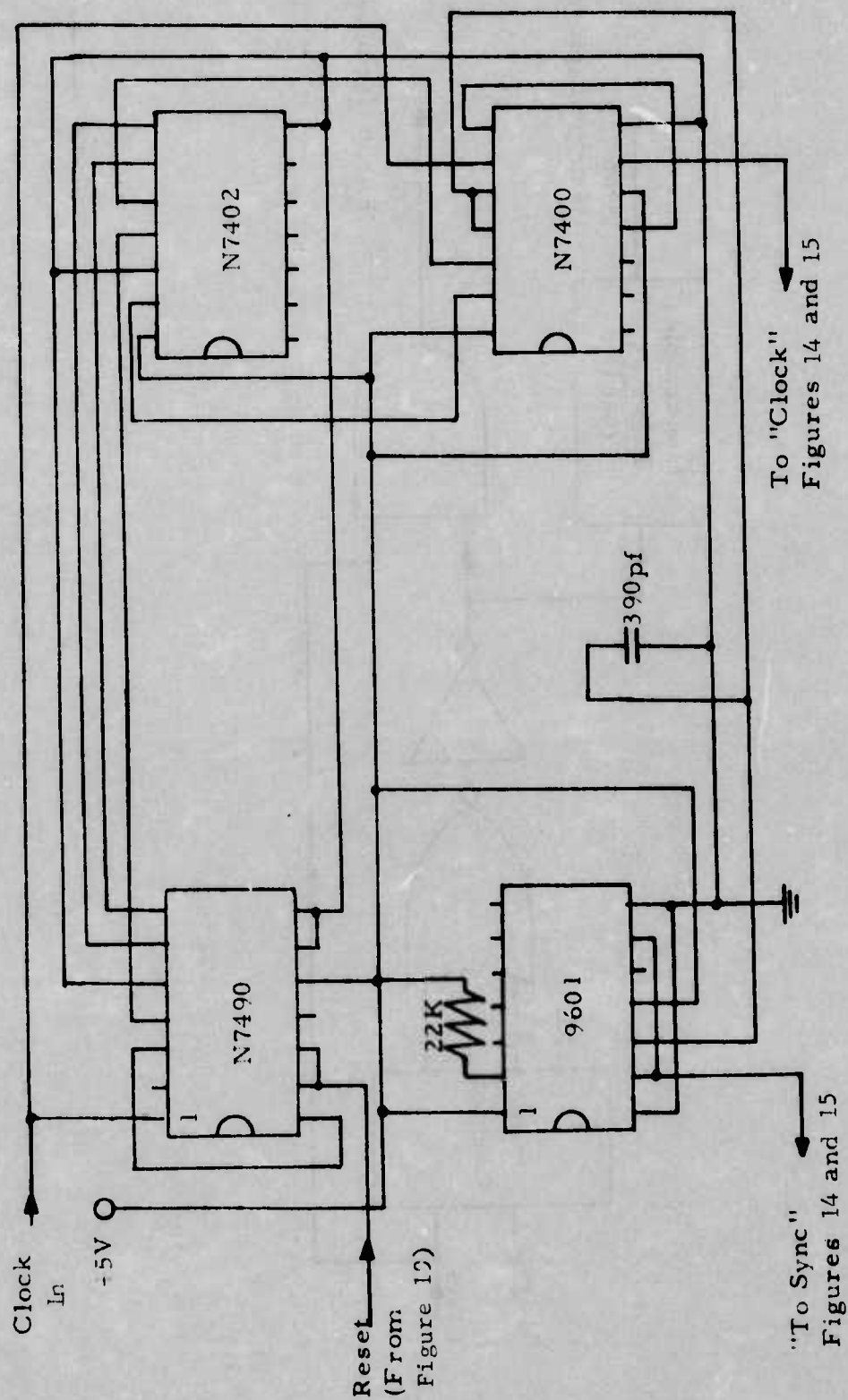Figure 21. Gating Network Used in the Continuous Scan Mode.

45

Figure 22. Gating Network Used in the Continuous Scan Mode.

46

The N7400 quad TTL NAND gate and the N7402 quad TTL NOR gate integrated circuits were used to generate the gating functions of Figure 21. An oscillogram of the output of the ramp voltage network is shown in Figure 23.

An abbreviated diagram of the DBFSR when operated in the continuous sweep mode is shown in Figure 24. It is seen here that the Gunn source is now being tuned by the ramp waveform, and the clock is synchronized to the NE566 ramp oscillator. Also, the multiplexer logic is now receiving clock pulses and sync pulses from the gating network.

9. LONGITUDINAL SHUNT-SLOT ARRAYS

Originally, the four arrays of the DBFSR were all of the narrow wall shunt-slot (edge slot) type (Reference 2). For the modified system, both the receiving and transmitting arrays for the elevation plane were replaced by arrays constructed with longitudinal broad-wall shunt-slots. This was done in order to have like polarizations for both the azimuth and elevation scans.

For the arrays of the DBFSR, a Taylor distribution was used in determining the excitation current amplitudes. The mainlobe to sidelobe ratio was specified as 25 dB. Once the excitation current amplitudes are specified, the conductance required for each slot in the wall of the guide is calculated (Reference 5). These slot conductances are then used to determine the physical dimensions of the slot.

The data needed to determine the slot dimensions from slot conductances is provided in Reference 8, where experimental test data are given for 1/16 inch slots in RG-52/U waveguide. There were essentially two parameters which had to be determined for each slot (Figure 25): (1) the displacement, x, of the slot from the center of the waveguide wall and (2) the length, y, of the slot for 9.0 GHz resonance. The resonant length of the slot is a function of the displacement x. The slot spacing down the center of the guide is specified in the original design as 0.8 inch. This is the distance from the center of one slot (along the length of the slot) to the center of an adjacent slot.

The conductance of a longitudinal shunt slot is given by (Reference 8):

$$G = A \sin^2 (\pi x/a) \tag{10}$$

Reference
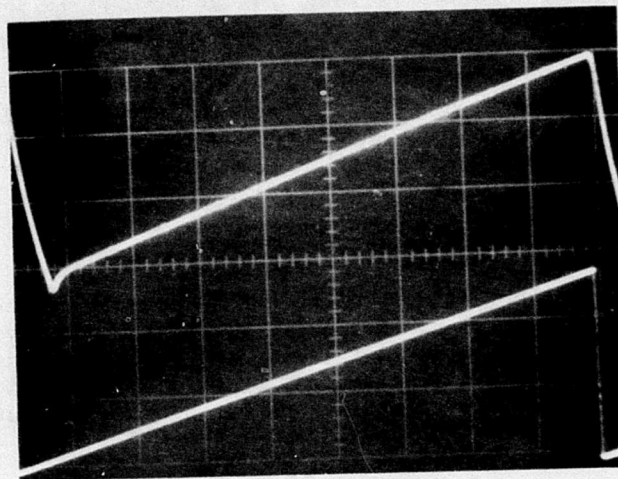8. Jasik, Henry. Antenna Engineering Handbook. New York: McGraw Hill Book Co., Inc., 1961.

Figure 23. Ramp Tuning Voltage (Upper Trace;
Vertical Scale = 5V/Div., Horizontal
Scale = 5μs/Div.) and the Corresponding
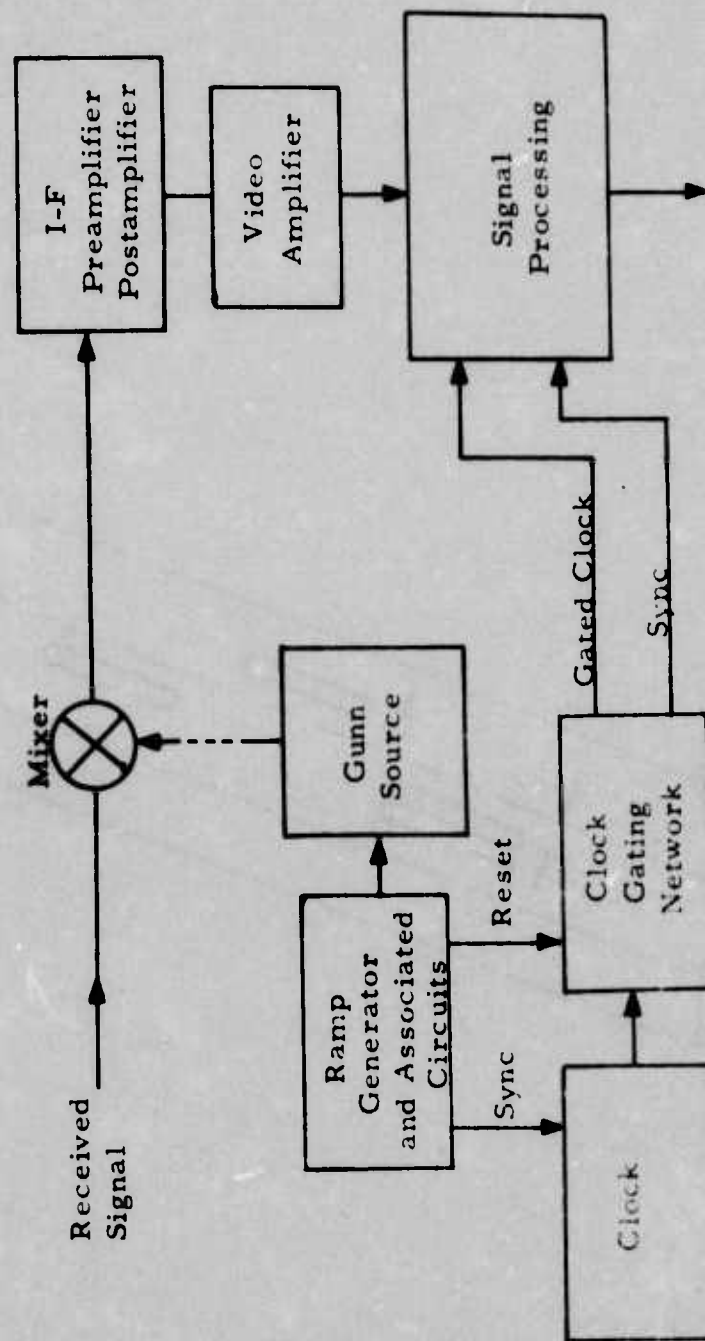Input to the Ramp Amplifier Network
(Vertical Scale = 2V/Div.).

Figure 24. One Receiver of the DBFSR Operating in the Continuous Scan Mode.
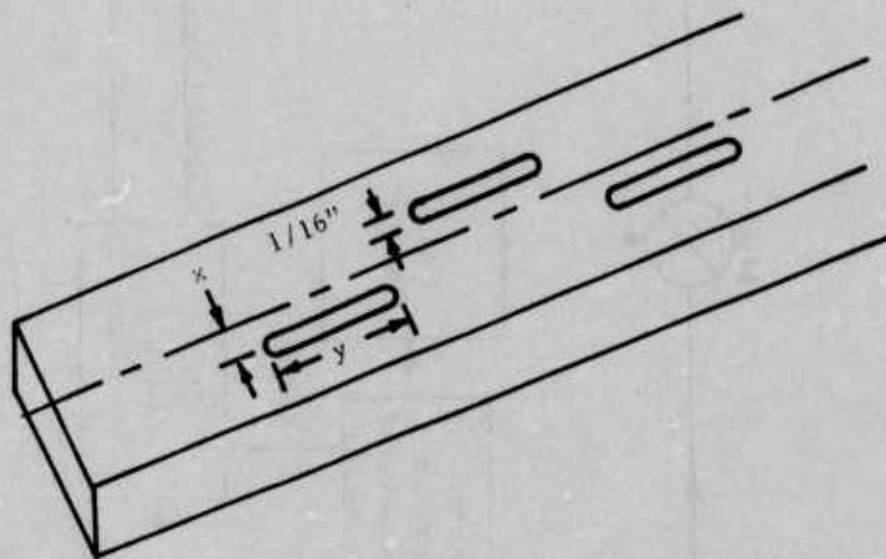
49

Figure 25. Slot Geometry in the Broadwall of a Waveguide Section.

Where:

G is the normalized resonant slot conductance.

A is the proportionality constant.

x is the slot displacement from center of guide wall.

a is the inside dimension of the broad wall of the guide, which equals 0.9 inch for RG-52/U waveguide.

The value of A is found by substituting, into Equation 10, a value of 0.53 mhos for G at x = 0.1833 inch and at a frequency of 9.0 GHz (Reference 8). Then Equation 10 can be put in an alternate form:

$$x = (a/\pi) \sin^{-1} (G/A)^{1/2} \qquad (11)$$

The required conductances can be substituted into Equation 11, and the displacement for each slot can then be calculated. Once the displacement for each slot is known, the slot length for resonance at 9.0 GHz can be determined from graphical data of Reference 8. The results of these calculations are given in Table 3.

Slots were milled into RG-52/U brass waveguide, and the array sections were trimmed to the proper length, with a flange mounted to one end of each section. The other ends were fitted with specially constructed terminations that acted as a load at the end of the array (Reference 5). Then, the completed arrays were tests for efficiency and for the visual standing wave ratio (VSWR) in the laboratory. The results of these tests indicated that the VSWR of the arrays ranged from 1.02 to 1.075 as the frequency was varied from 8.5 to 9.5 GHz. These values were well within acceptable limits. The efficiency of the arrays was measured by a substitution method wherein a power meter is calibrated for a certain power flow, and the amount of power which is lost upon inserting the array in the line is noted. In performing this test, the substitution of the arrays in the line resulted in 80 percent loss of power. This indicated that the array is absorbing or radiating 80 percent of the power fed to its input. Allowing 5 percent wall losses in the guide, this can be interpreted as a 75 percent radiation efficiency for the array, which is the design specification.

TABLE 3

Construction Data for 36 Element Broad Wall

Shunt Slot Array in RG-52/U Waveguide

(1/16 inch slots, 0.8 inch spacings)

Slot No.	Displacement, x (inches)	Slot Length, y (inches)
1	0.017	0.633
2	0.018	0.634
3	0.019	0.634
4	0.020	0.634
5	0.022	0.634
6	0.025	0.634
7	0.028	0.634
8	0.031	0.635
9	0.034	0.635
10	0.038	0.635
11	0.041	0.635
12	0.045	0.635
13	0.048	0.636
14	0.051	0.636
15	0.054	0.636
16	0.057	0.636

TABLE 3 (Continued)

Slot No.	Displacement, x (inches)	Slot Length, y (inches)
17	0.060	0.636
18	0.062	0.636
19	0.065	0.636
20	0.068	0.636
21	0.070	0.637
22	0.072	0.637
23	0.074	0.638
24	0.075	0.639
25	0.076	0.638
26	0.076	0.638
27	0.075	0.638
28	0.073	0.637
29	0.070	0.637
30	0.070	0.637
31	0.064	0.636
32	0.060	0.636
33	0.057	0.636
34	0.055	0.636
35	0.054	0.636
36	0.054	0.636

10. TOWER TESTING OF THE FREQUENCY SCANNED RADIOMETRIC SYSTEM

On 29 June 1973, the Frequency Scanned System was deployed on the roof of Building 11 at Eglin AFB (Figure 26). A trihedral corner reflector having an apparent cross section (at x-band) of 600 m^2 was deployed at approximately 1700 feet slant range on the ledge of the fuze test tower. A section of absorbing material (Eccosorb) was used to alternately cover and uncover the reflector while the response of the system was noted. The reflector was at times rotated back and forth on a vertical axis to observe the effect on system response. Both azimuth and elevation channels could detect the rotation and shielding of the reflector. Since the reflector was only slightly above a nearby tree line, some problems were experienced due to the sudden transition from tree return to cold sky. There was evidence that the tower was being detected while the reflector was shielded from the system. During this test, the multiplexing and integrating circuitry was in a bread-boarded form (Figure 27), and the original stairstep voltage and clock generating circuitry were being used.

It was decided that both a faster clock rate and a better rise time for the stairstep voltage transitions were needed, so the presently existing stairstep generator (D/A converter) and clock circuitry were designed, built, and tested. The completed stairstep generator circuit board was mounted above the old stepper circuitry, and the new clock circuitry was fastened to the rear of the system mounting board, along with the now completed multiplexer-integrator circuit board.

On 18 July 1973, the system was again deployed on the roof of Building 11, and the 660 m^2 corner reflector was placed on the fuze test tower. The response of the system proved to be markedly superior to that displayed in the previous test. First, the original or internal clock was used at an 8 Hz rate, and variations of almost 2 volts were observed in the output of the integrator as the reflector was covered and uncovered (Figure 28). Similar results were obtained with the faster rate of the newly built clock. The faster clock rate (240 Hz) produced a sweep rate of 20 Hz. Video tapes and still photos were taken during this test.

In using a fast clock rate, it was discovered that rapid stepping of the VCO generated spurious signals in the output of the mixer-preamplifier module. Further investigation revealed that these high level signals were low-frequency in character (8 to 25 MHz). To combat this problem, the inadequate filtering of the i-f amplifier was supplemented by the addition of a discrete component, single pole, LC high pass filter at the input of the postamplifier, providing a 3 dB point of 50 MHz. The additional filtering proved adequate as a temporary measure, but a coaxial filter was ordered shortly thereafter.
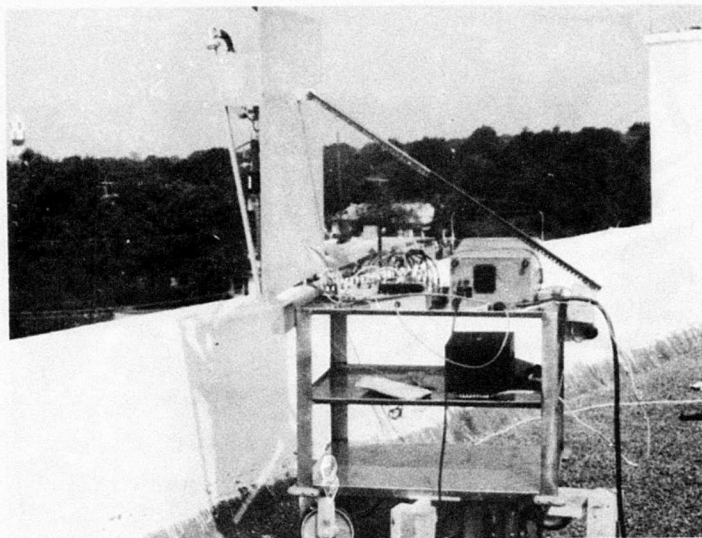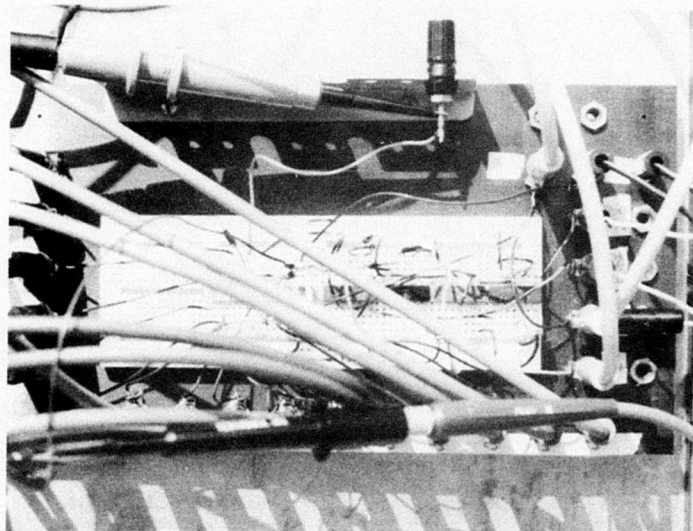
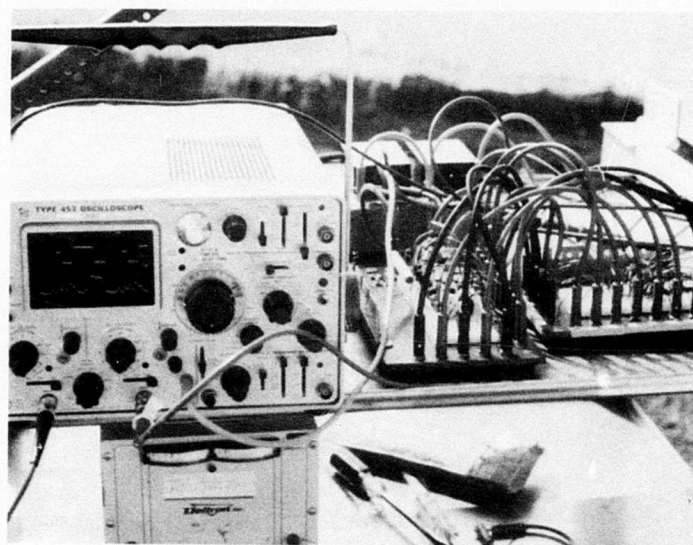(a) Frequency-Scanned System as deployed on the roof of Building 11.
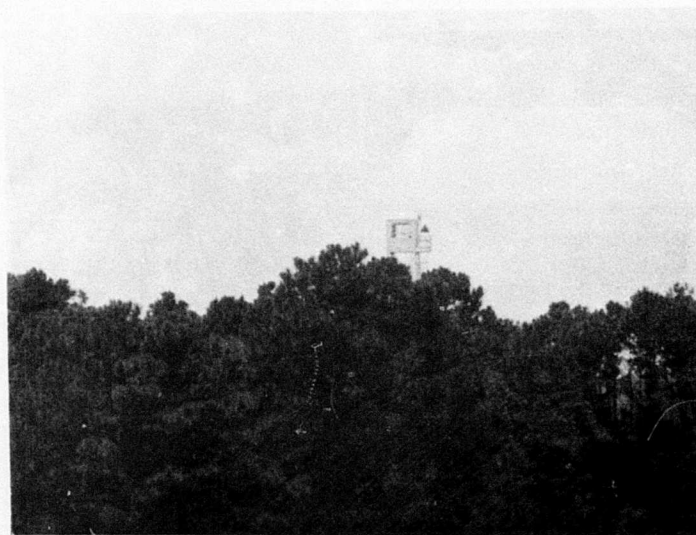
(b) Telephoto view of 660 m^2 corner reflector deployed on the ledge of the fuze test tower. (Approximate range is 1700 ft)

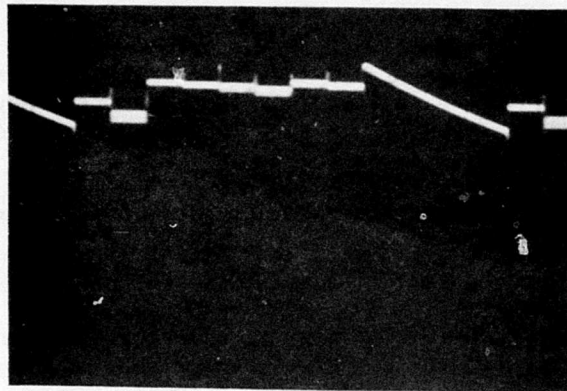Figure 26. Setup for First Tower Test.

55

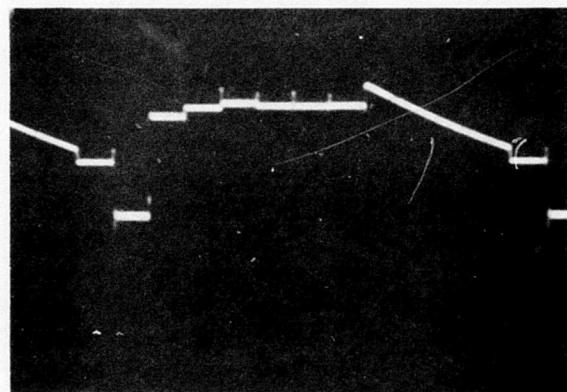(a) Overhead view of multiplexer circuit breadboard.

(b) Multiplexer and integrator breadboards.

Figure 27.   Circuit Breadboards for First Tower Test.

56

(a) Reflector covered.

(b) Reflector uncovered.

Figure 28.   Multiplexed Integrator Output.

57

The existence of a ringing problem in the mixer suggested the use of a continuous scan, which would free from jumps in frequency except for the flyback interval. Therefore, a ramp tuning voltage was implemented to test this idea.

On 16 August 1973, the system was deployed on the ledge of a former aircraft control tower at Eglin AFB, and the 660 m^2 corner reflector was positioned in an adjacent field (Figure 29).

Tests were performed for the corner reflector at a range of approximately 1200 feet from the tower. First, the elevation channel was tested for the continuous scan (ramp) mode. Oscillograms for the output of the video amplifier, along with the VCO voltage, are shown in Figure 30 for the corner reflector being shielded and unshielded with absorbing material. In this test, a sweep frequency of 22.2 Hz resulted in the maximum received signal for the video amplifier output, and from Equation 3:

$$\Delta f / \Delta t = (9.5 - 8.5) \ 10^9 / (1/22.2 \times 10^3) = \tag{12}$$

$$22.2 \times 10^{12}$$

Therefore, from Equation 5, for a 50 MHz i-f cut-off frequency:

$$t_p = 50 \times 10^6 / 22.2 \times 10^{12} = 2.25 \ \mu s \tag{13}$$

From Equation 4, this yields a minimum distance of:

$$d = (1/2) \ (3 \times 10^8) \ (2.25 \times 10^{-6}) = 337.5 \ \text{meters} = \tag{14}$$

$$1107.3 \ \text{feet}$$

These calculations have assumed a linear variation of the VCO with the tuning voltage.

In Figure 31, the multiplexed integrator outputs of Figure 13 are shown. These outputs result from the video signals shown in Figure 30 for the reflector being shielded and unshielded.
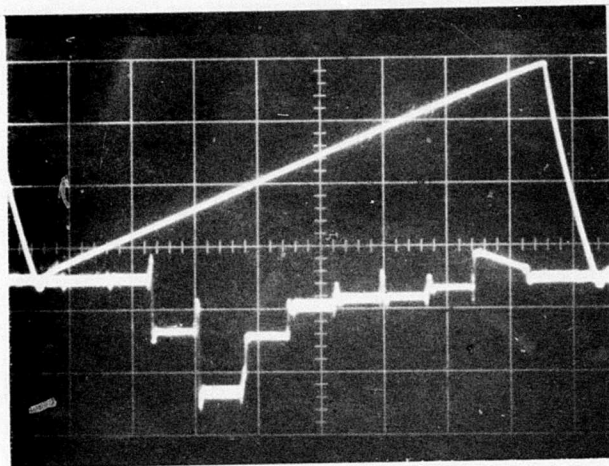
(a) Frequency-Scanned System deployed on ledge of former control tower.
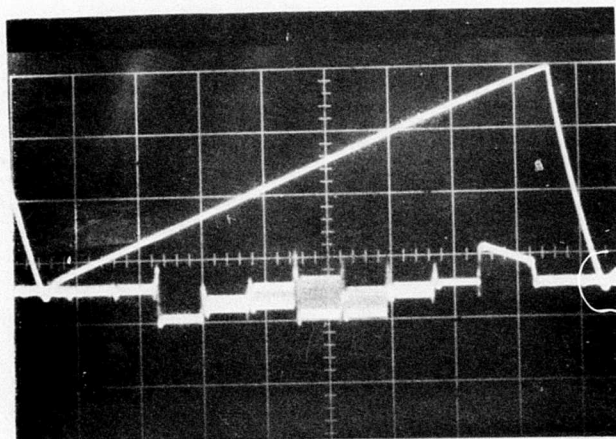

(b) Telephoto view of 660 m^2 corner reflector at approximate range of 1200 feet.
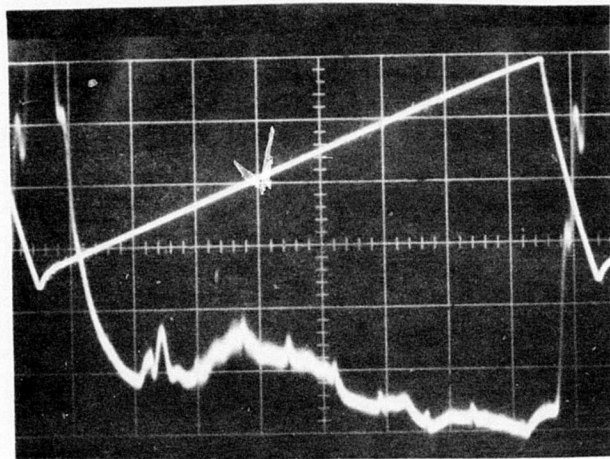
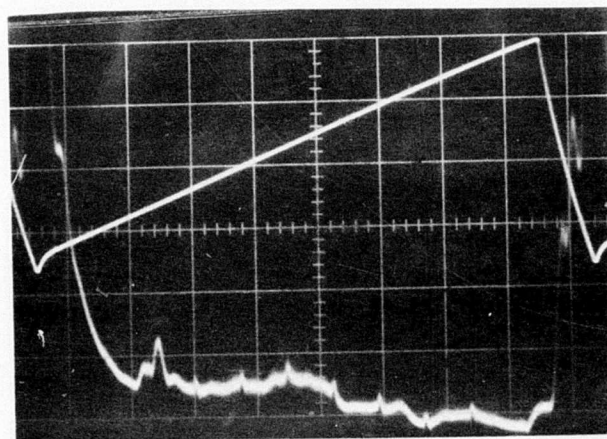Figure 29. Test Setup for Second Tower Test.

(a) Reflector unshielded.

(b) Reflector shielded.

Figure 30. Ramp Tuning Voltage (Upper Traces).

60

(a) Ramp voltage and integrator output with
reflector unshielded.

(b) Ramp voltage and integrator output with
reflector shielded.

Figure 31. Multiplexed Integrator Output for the Video Inputs of Figure 30.

61

Figure 32 shows the oscillograms for the identical test for the
azimuth (vertical fan beam) channel. In this figure, the video amplifier
output and multiplexed integrator output are shown for the unshielded
corner reflector.
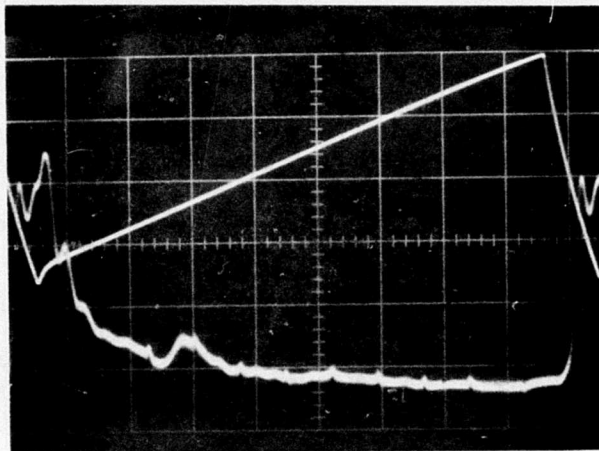
(a) Ramp voltage and video.
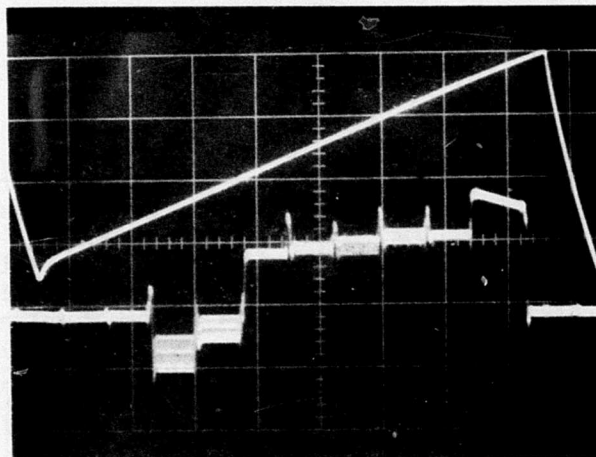
(b) Ramp voltage and multiplexed integrator
    output.

Figure 32. Video and Multiplexed Integrator Output for Azimuth Receiver.

SECTION IV

ADDITIONAL MODIFICATIONS TO THE

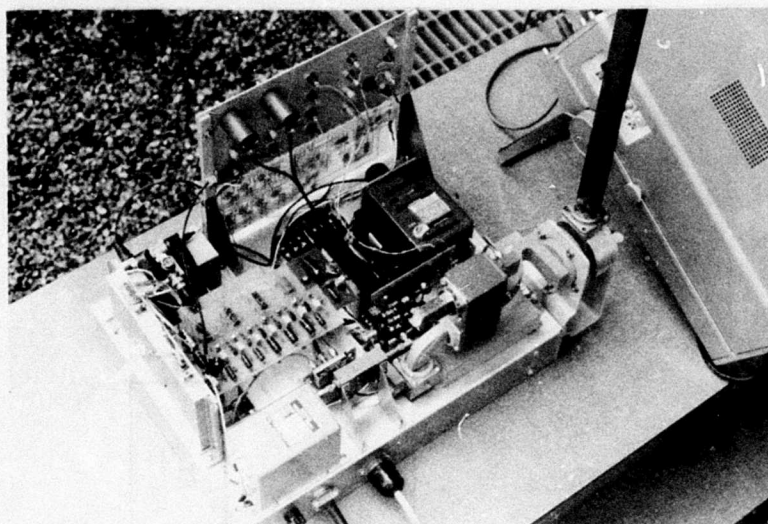## DUAL-BEAM FREQUENCY-SCANNED RADIOMETER

Between September 1973 and July 1974, the DBFSR was reconstructed into a modified system consisting of a single channel radiometric receiver. The Modified Dual-Beam Frequency-Scanned Radiometer (MDBFSR) was designed such that the two-dimensional scan would be achieved by multiplexing two frequency-scanned antenna arrays at the input to the receiver. Gating of the receiver and r-f switching permit the use of each array as both a receiving and a transmitting antenna. The receiver gating circuitry was designed to provide an effective range gate network for the system.

Another modification of this system would employ the use of a 20 x 20 element frequency-scanned array that was designed and constructed in a previous program (Reference 5). The feed system for this array has been altered to allow for insertion of a dielectric vane. This permits a method of mechanically scanning the antenna beam at an angle of 45 degrees to that due to frequency-scanning. This results in a two-dimensional scan for this array by the use of a combination of frequency and mechanical scanning. When the system is used in this configuration, it is referred to as the Single-Channel Dual-Scan Radiometer (SCDSR).

1. SYSTEM DESCRIPTION OF THE MODIFIED DUAL-BEAM FREQUENCY-SCANNED RADIOMETER (MDBFSR)

The prototype model of the MDBFSR is shown in Figure 33. A block diagram of the system is given by Figure 34. The tuning voltage and logic circuits are omitted because they remain essentially unchanged from the original system when operated in the stepped mode described in Section III. The circuit elements associated with the ramp mode were not incorporated into this system. In addition, only one antenna has been used to generate a single beam scan for the initial evaluation of the prototype system.

The r-f output of the Gunn VCO is fed to a 10 dB directional coupler (Microlab Model CB-87F), which couples -10 dB of r-f energy into the local oscillator input port of the mixer. The output port of the directional coupler is connected to the input of a SPDT microwave switch (PRF Model 5-2G-1). This switch is controlled by a TTL logic pulse supplied by the range gate circuitry. A high logic state results in r-f power being delivered to a four-port circulator (E&M Laboratories Model X-104 LTD), whereas a low state sends the power to a 50 ohm termination. The r-f power is coupled through the circulator to the antenna for transmission. A waveguide rotary joint was installed between the circulator and the antenna to allow movement of the array.

64

(a) Top view.
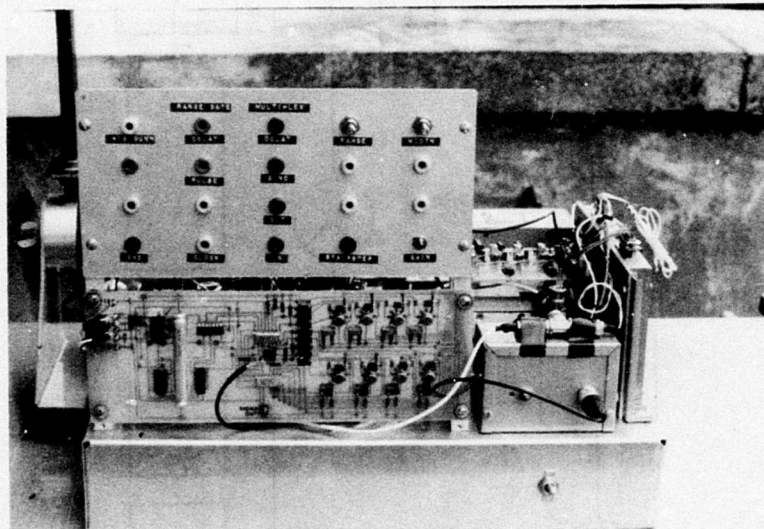
(b) Front view.

Figure 33. Configuration of Modified Dual-Beam Frequency-Scanned Radiometer.
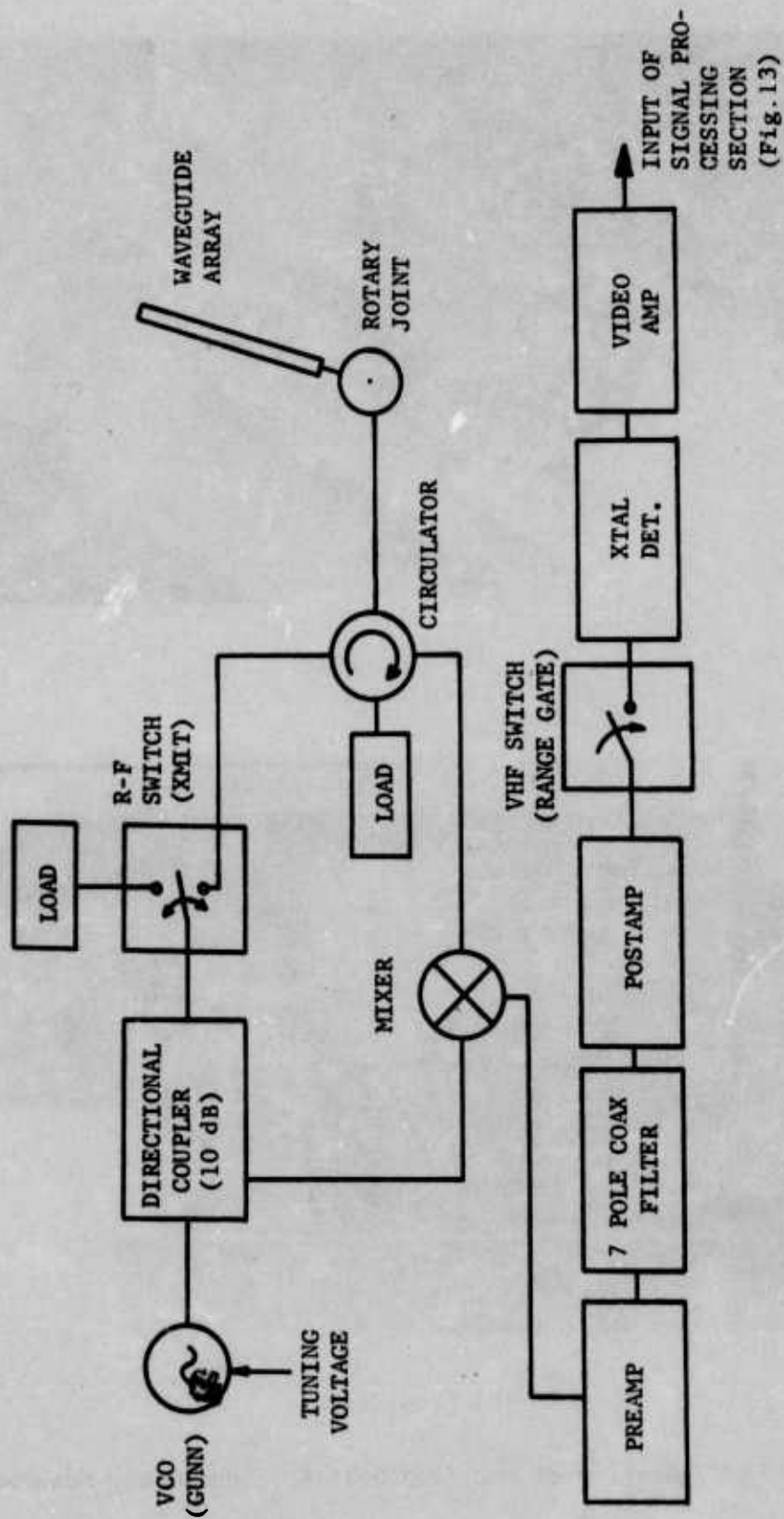
65

Figure 34. Modified Dual-Beam Frequency-Scanned Radiometer.

66

The remaining two ports of the circulator are connected such that the energy received by the antenna array will be directed to the mixer input port with any reflections being delivered to a matched termination on the fourth port. Frequency conversion takes place in the mixer and the amplified signal appears at the output of the mixer-preamplifier module. This output is fed to a seven pole high-pass coaxial filter (CIR-Q-TEL Model FHT/7-46-7/50-28A/28A) having a cut-off frequency of 50 MHz. This filter was necessary to eliminate spurious signals at approximately 10 MHz, which are generated by the mixer-preamplifier module in the stepped-mode of operation. The filter output is then fed to the postamplifier input.

The postamplifier and the detector of the original DBFSR were found to have two undesirable operational characteristics. The latter two gain stages of the postamplifier tended toward saturation, resulting in signal distortion, and the detector had a rather poor high frequency response. The first of these problems was eliminated by bypassing the last two gain stages of the postamplifier to the input of a new amplifier (Avantek UTA-544M/B) having 28 dB of gain. The output of this amplifier was then fed to a SPST VHF switch (LORCH Electronics Model ES-216 D). This switch is controlled by a TTL logic level pulse from the range gate network. A low logic state causes the VHF switch to close and allows the i-f signal to reach the detector, whereas a high logic state blocks the signal. The crystal detector (HP Model 423A) that follows this switch replaces the original square-law detector incorporated in the postamplifier module. The high frequency response of this detector is greatly superior to that of the original square-law detector. Figure 35 compares the detector output voltage taken from the original system with that from the modified system for an identical input to the system. The gain of the modified network is approximately 10 times that of the previous system with a greatly improved high frequency response.

The system beyond the detector is essentially unchanged from that described in Section III. The video amplifier provides additional gain after the detector, and the signal processing circuits (Figure 13) then operate on the video amplifier output.

2. RANGE GATE CIRCUITRY

The logic circuitry of the previous DBFSR configuration was altered by the addition of the range gate circuitry which is required to control the VHF and r-f switches in the modified system. This change consists of the addition of monostable multivibrators into the timing network as shown in Figure 36. In this configuration, a sequence of events occurs as shown by the timing diagram of Figure 37. In this diagram, the leading edges of the clock pulses trigger monostable multivibrator
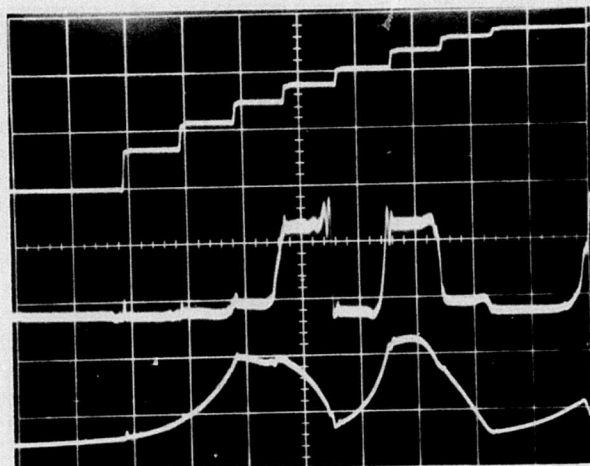
67

Figure 35. Response of the Original Square-law Detector (Upper), the
           Crystal Detector of the MDBFSR (Center), and the D/A Voltage.
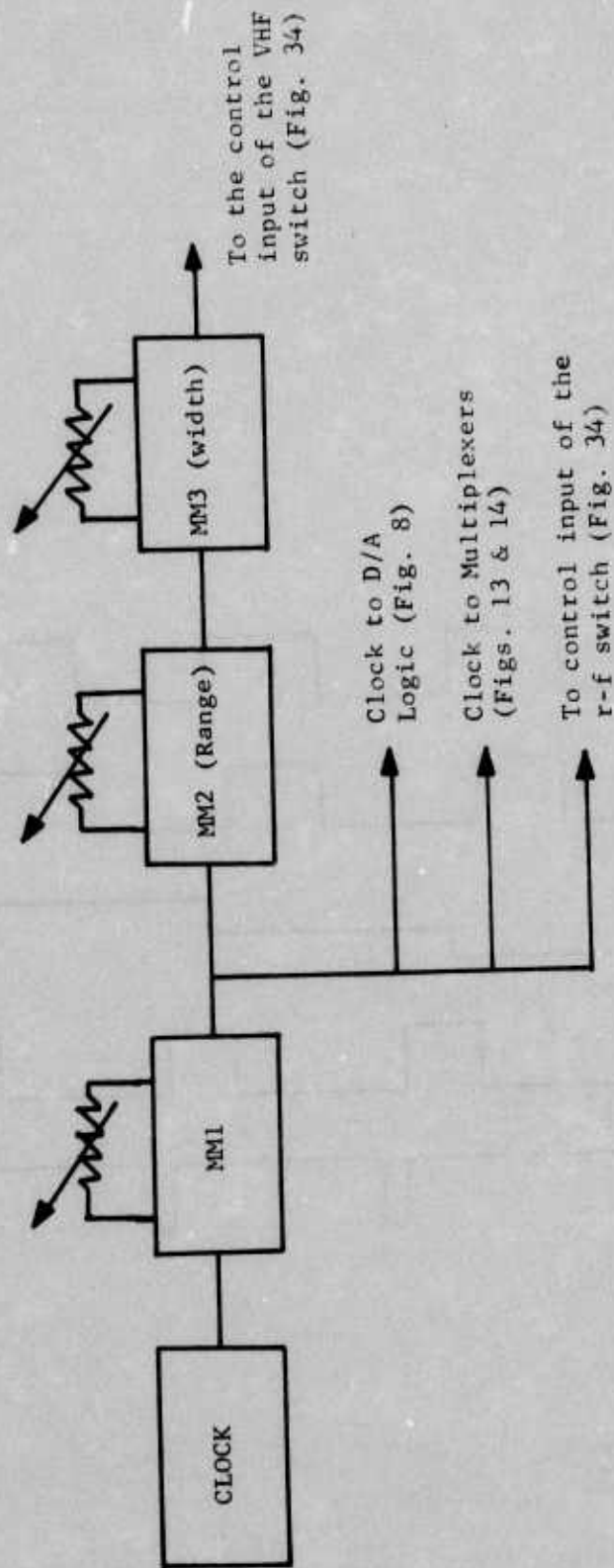   (Vertical scale: 20 mV/div upper and 200 mV/div center.)

Figure 56. Range Gate Circuit of the Modified Dual-Beam Frequency-Scanned Radiometer (MDBFSR).
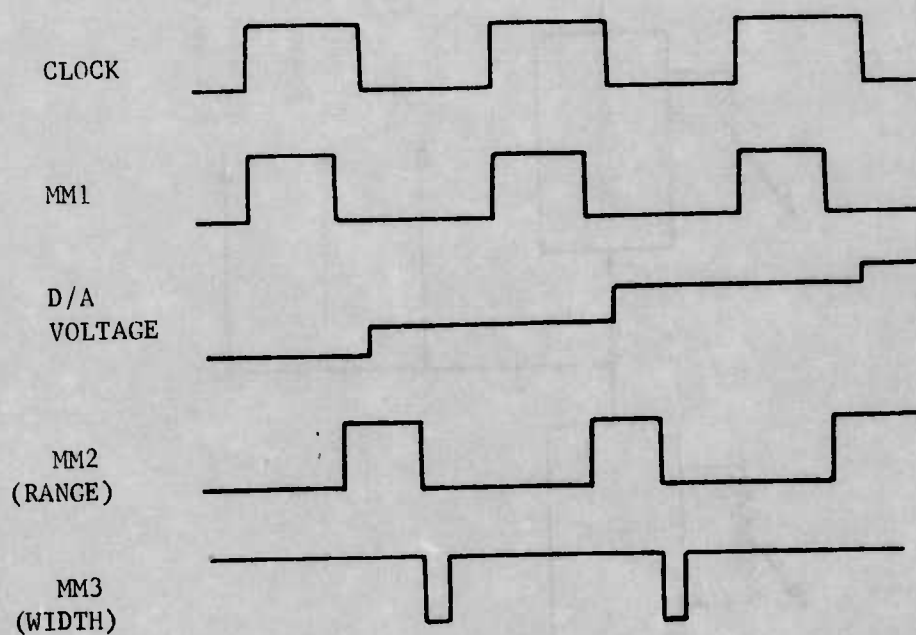
Figure 37. Timing Diagram for the Range Gate Network of the MDBFSR.

1 (MM1) of the range gate circuit. The output of MM1 is then used to clock the remaining logic circuits. During the high state of MM1, the r-f switch is set such that the system is transmitting during this interval. A potentiometer is provided in the timing circuit of MM1 to allow adjustment of the length of the transit time interval.

The trailing edge of MM1 output pulse triggers the range monostable multivibrator (MM2) which in turn triggers the width monostable multivibrator (MM3). The output of MM3 is the control pulse for the VHF receiver switch. The timing circuits of MM2 and MM3 include ten-turn potentiometers (30 kilohm) to permit precise adjustment of the range and width time intervals. These potentiometers are mounted to the control panel of the system.

An advantage of the timing sequence shown in Figure 37 is the separation of the transmit and receive intervals. This allows transients due to switching of the r-f section to subside and greatly reduce interference with the received signal. An oscillogram of the stairstep voltage, the r-f switch control pulse (MM1 output), and the VHF switch control pulse (MM3 output) is shown in Figure 38. The clock rate in this case is approximately 240 kHz.

The three monostable multivibrators employed in the range gate circuit are type N74121 TTL integrated circuits. The schematic for this network is shown in Figure 39.

3. PRELIMINARY TOWER TESTING

During the course of experimental work with the MDBFSR, the receiver range gate switch (VHF switch) was electrically damaged and failed to operate properly. This failure made it impossible to perform a tower test using the range gate circuits. Furthermore, without the use of the VHF switch to eliminate the r-f switching transients, it was impractical to operate the r-f switch.

Prior to the failure of the VHF switch, extensive laboratory work was devoted to developing the ranging system, with promising results during laboratory testing. It was found that the noise due to r-f switching was originating primarily in the mixer and could be almost completely eliminated by placing isolators in the input lines to the mixer. This improvement will be incorporated into the system when coaxial isolators can be obtained.

During June 1974, the MDBFSR was deployed on the antenna deck of the Electrical Engineering Building at Louisiana State University (Figure 40). A large crane, which was at an approximate range of 1000 feet, was chosen as a target of adequate cross-sectional area. In this test, it was necessary to use a horn antenna for illumination since the VHF switch was not operable to block the switching transients appearing in the i-f signal. For receiving purposes, a 50 element frequency-scanned slotted-waveguide antenna array was utilized (Reference 5). A standard gain horn (16 dB gain)
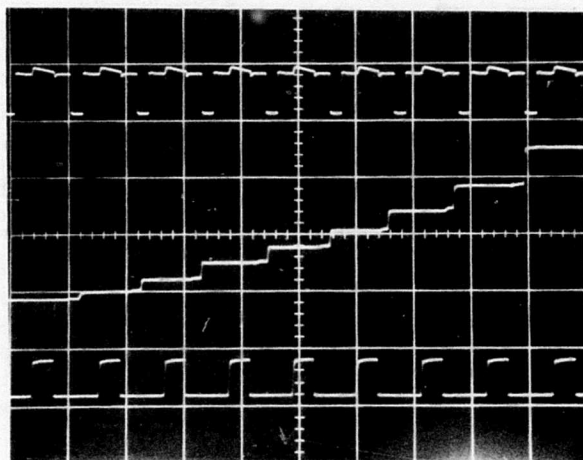
Figure 38. Range Gate Network which Controls the VHF Switch
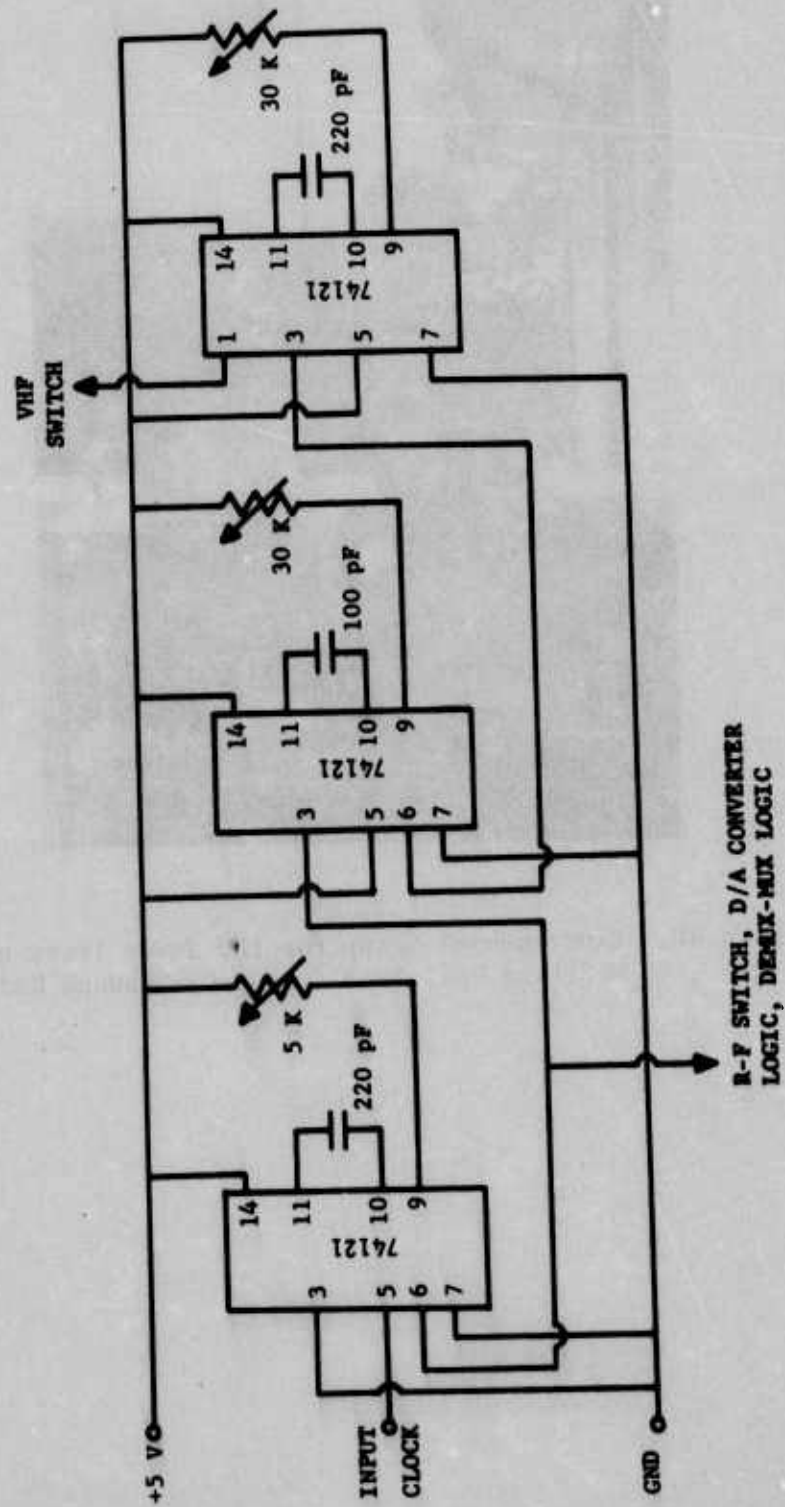(Upper), D/A Voltage (Center), and R-F Switch (Lower).
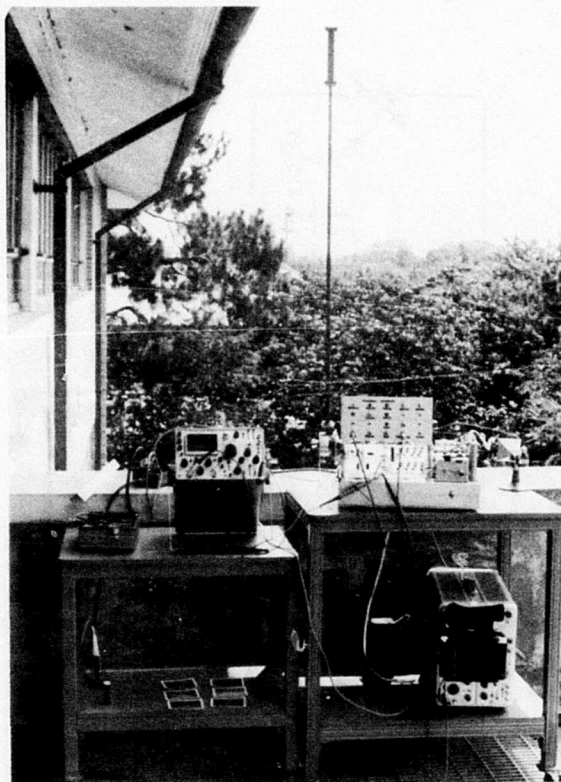
Figure 39. Range Gate Circuit.

Figure 40. Experimental Setup for the Tower Tests of the
Modified Dual-Beam Frequency-Scanned Radiometer.

74

was oriented in the direction of the crane, and the receiving array was positioned such that its main beam would scan vertically (elevation) from a point below a nearby tree line to a point above the crane. The block diagram for the system as it was operated during this test is shown in Figure 41.

The oscillograms of Figure 42 illustrate the response of the system at Output A of Figure 41 for this test. The results shown were taken with the r-f switch held in a static condition such that the horn illuminated continuously during each time interval in the stairstep VCO input voltage. Figure 43 shows the results for a similar test for Output B of Figure 41. An indication of a return signal from the nearby tree line is also visible in this figure. This would have been eliminated if the range gate network had been operational.

4. SINGLE-CHANNEL DUAL-SCAN RADIOMETER

Another configuration similar to that of the MDBFSR is the Single-Channel Dual-Scan Radiometer (SCDSR). The block diagram for this system is the same as that of Figure 34, with the following exceptions:

     (a) The multiplexed dual-beam antennas are replaced by a 400-element frequency-mechanically-scanned planar array.

     (b) An additional demultiplexer/multiplexer network with integrators is required for each mechanically controlled beam pointing position.

The most important component in this system is the antenna network. The design and construction of a frequency scanned 20 x 20 element planar array was performed in a previous program (References 5 and 9 to 11). This array can be modified by incorporating a mechanically controlled dielectric vane in the feed system of the array in order that a two-dimensional scan is obtained. Insertion of a dielectric vane in the feed system results in a phase delay of the wave propagating in the feed structure. This delay is proportional to the width and depth of the dielectric vane and to the relative dielectric constant of the vane.

Reference

9. Hilburn, J. L. and F. H. Prestwood. "K-Band Frequency-Scanned Waveguide Array". IEEE Trans. on Antennas and Propagation, Vol. AP-22, No. 2. March 1974.

10. Raffoul, G. W. and J. L. Hilburn. "Radiation Efficiency of an X-Band Waveguide Array", IEEE Trans. on Antennas and Propagation, Vol. AP-22, No. 2. March 1974.

11. Hilburn, J. L., et. al. "Frequency-Scanned X-Band Waveguide Array", IEEE Trans. on Antennas and Propagation, Vol. AP-20, No. 4. July 1972.
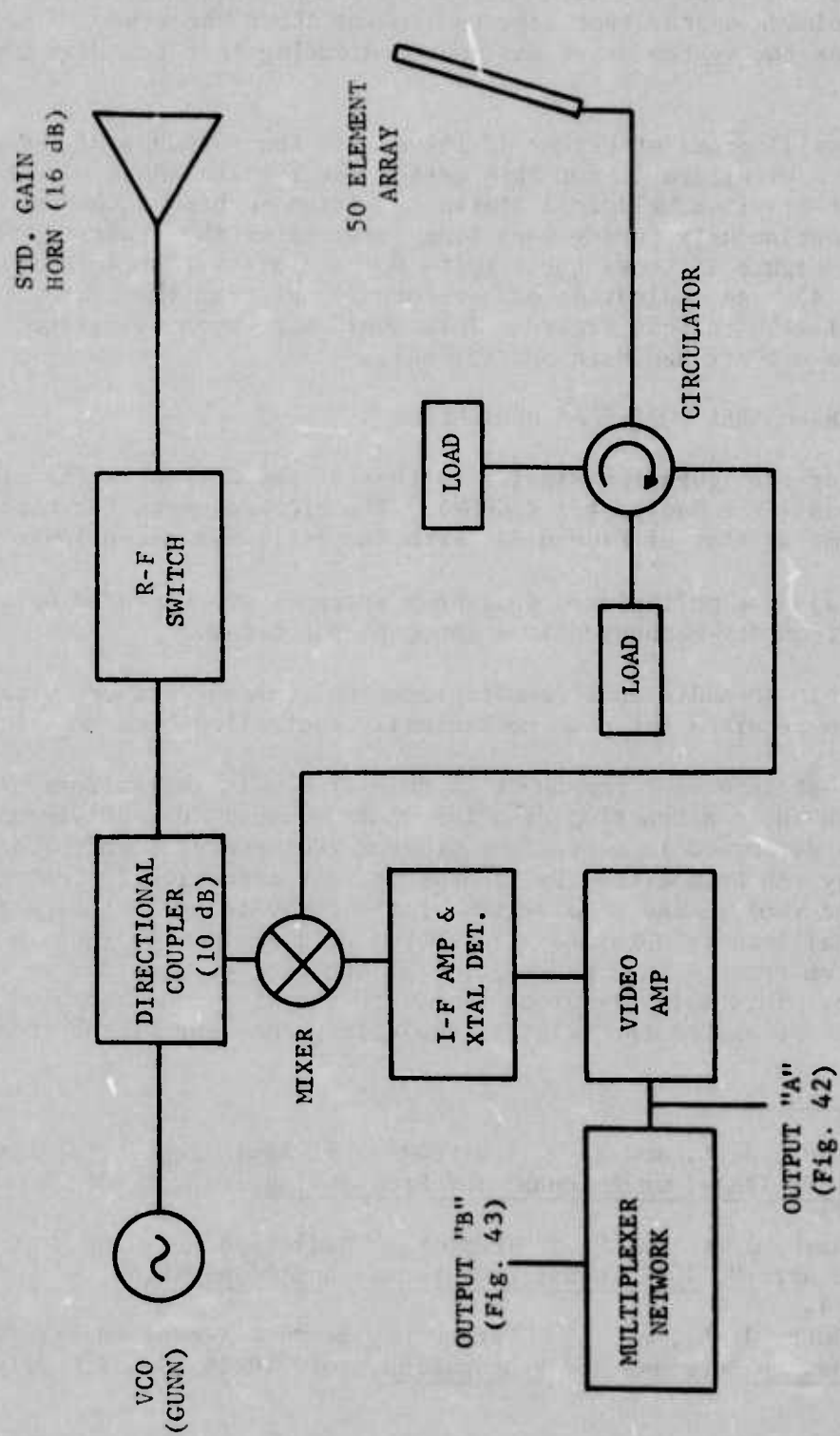
Figure 41. Modified Dual-Beam Frequency-Scanned Radiometer (MDBFSR) Employed in the Tower Tests.
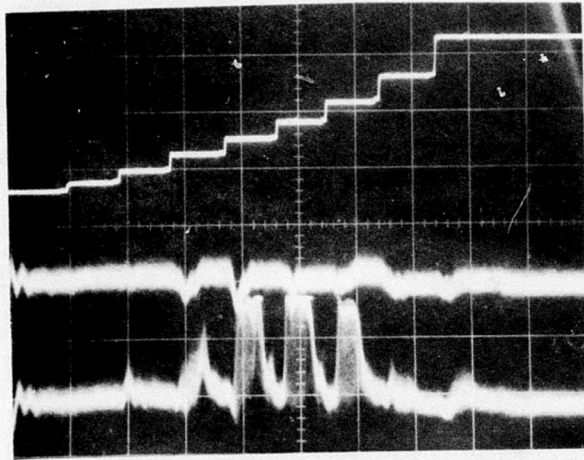
76

Figure 42. Video Response for Tower Test on Crane for
No Illuninator Power (Middle) and for
Illuminator Power (Lower). Top Waveform
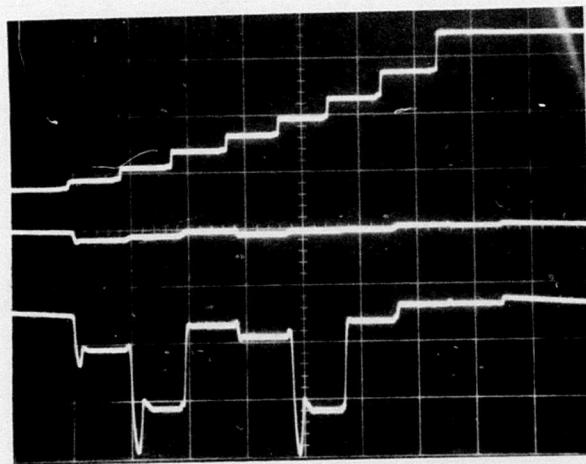is the VCO Input Voltage.

Figure 43. Multiplexed Integrator Output for Tower Test
on Crane for No Illuminator Power (Middle) and
for Illuminator Power (Lower). Top Waveform is
the VCO Input Voltage.

The geometry of the vane in the feed system to be employed is shown in Figure 44. For this geometry, the y-components of the electric field intensity and the z-components of the magnetic field intensity for regions 1 and 2 within the waveguide are:

$$E_{y_1} = -j \ \frac{k}{k_1} \sqrt{\frac{\mu_o}{\varepsilon_o}} \ C_1 \sin k_1 x \ , \quad 0 \leq x \leq \frac{a-t}{2} \quad (15)$$

$$E_{y_2} = -j \ \frac{k}{k_2} \sqrt{\frac{\mu_o}{\varepsilon_o}} \ C_2 \cos k_2 \left(\frac{a}{2} - x\right), \quad \frac{a-t}{2} \quad (16)$$

$$\leq x \leq \frac{a+t}{2}$$

$$H_{z_1} = C_1 \cos k_1 x \ , \quad 0 \leq x \leq \frac{a-t}{2} \quad (17)$$

$$H_{z_2} = C_2, \sin k_2 \left(\frac{a}{2} - x\right) \ , \quad \frac{a-t}{2} \leq x \leq \frac{a+t}{2} \quad (18)$$

Where:

$$k_1 = \sqrt{k^2 - \beta^2} \quad (19)$$

$$k_2 = \sqrt{k^2 \varepsilon_r - \beta^2} \quad (20)$$

$k = \omega \mu_o \varepsilon_o$ μ_o is the permeability of free space.

ε_o is the permittivity of free space.

$\varepsilon = \varepsilon_o \varepsilon_r \beta$ is propagation constant in the waveguide.

C_1 and C_2 are arbitrary constants.

A longitudinal-section electric mode exists when the boundary conditions for the tangential components of the electric and magnetic fields are satisfied at the dielectric interface (Reference 12). Equating Equation 15 to

Reference
12. Johnson, Curtis C. Field and Wave Electrodynamics. New York: McGraw Hill Book Co., Inc., 1965.

DIELECTRIC
VANE

RG 52/U
WAVEGUIDE

b

a
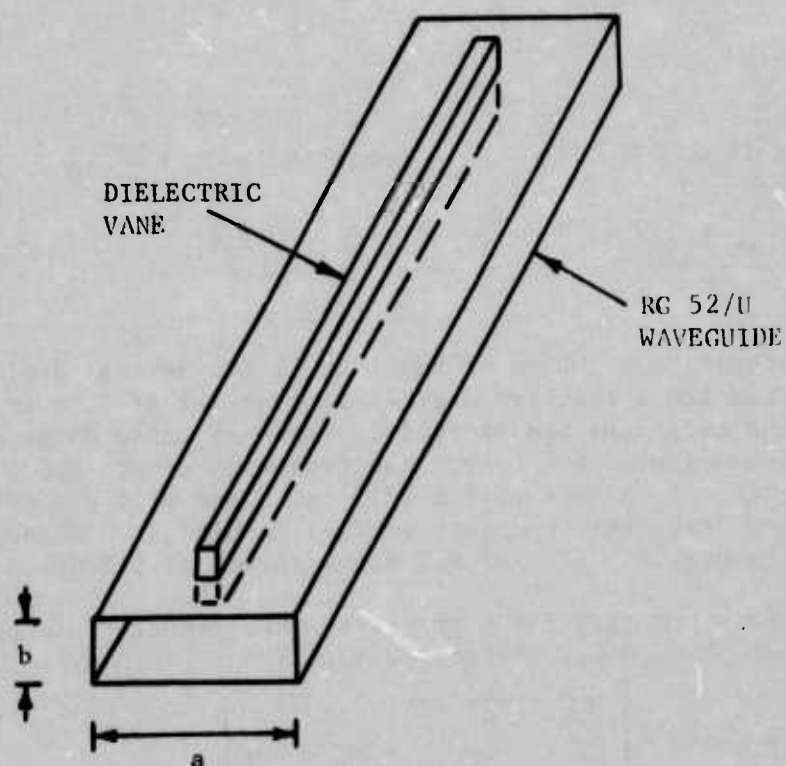
(a) Dielectric vane positioned
    in the feed system.

a/2   a/2

① ② ③

b

$\frac{a-t}{2}$ t
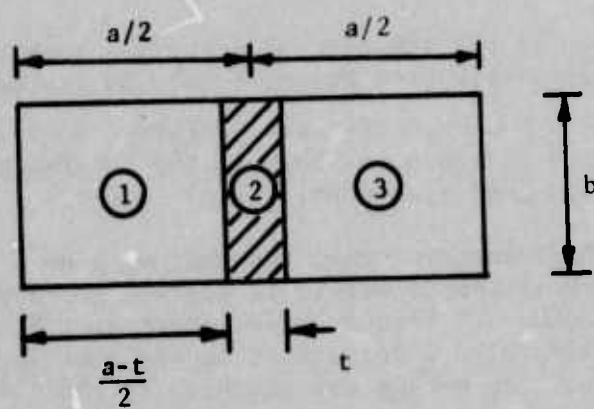
(b) Cross-sectional view of the
    dieletric vane in the waveguide.

Figure 44. Geometry of Dielectric Vane in Feed System.

Equation 16 and Equation 17 to Equation 18 at $x = \frac{a - t}{2}$ yields

$$\frac{\cot (k_2 t/2)}{k_2} = \frac{\tan [k_1 (a - t)/2]}{k_1} \tag{21}$$

An iterative solution of Equation 21 for several dielectric vane thicknesses and a relative dielectric constant of 2.54 is shown in Figure 45. These solutions are plotted in terms of phase delay along the feed section in degrees/inch versus the frequency of operation in GHz. From this figure, it is seen that a 1/12 inch vane of dielectric material with a relative dielectric constant of 2.54 results in a phase delay of 218 degrees/inch at 8.5 GHz and 265 degrees/inch at 9.5 GHz.

The beam pointing for a traveling wave structure in terms of the element-to-element phase delay (Reference 13) is:

$$\phi = \cos^{-1} \left[\sqrt{1 - \frac{\lambda}{2a}^2} + \theta_d - \frac{\lambda}{2d} \right] \tag{22}$$

Where λ is the free space wavelength, and θ_d is the additional phase delay introduced by the dielectric vane. In terms of the phase delay, Ψ, given in Figure 45, Equation 22, can be written as:

$$\phi = \cos^{-1} (\lambda \Psi / 9.144) \tag{23}$$

The feed section of the 400 element array was machined with a 1/12 inch slot, and a dielectric vane having $\epsilon_r = 2.54$ was mounted to this section (Figure 46). Measurements were performed to test the validity of the equations, and as shown in Table 4, the theoretical and experimental results are in good agreement.

For a 1/12 inch dielectric vane, the maximum scan from zero to full (0.4 inch) insertion is approximately 12 degrees for a given frequency between 8.5 and 9.5 GHz. A frequency deviation from 8.5 to 9.5 GHz results in a scan of approximately 15 degrees at an angle of 45 degrees to that of the mechanical scan. The mechanical scanning by the dielectric vane in

Reference
13. Wellman, W. J. and S. S. Shapiro. "Beam Pointing Direction of Traveling Wave Arrays", Microwaves, Vol. 8, No. 6, June 1969.
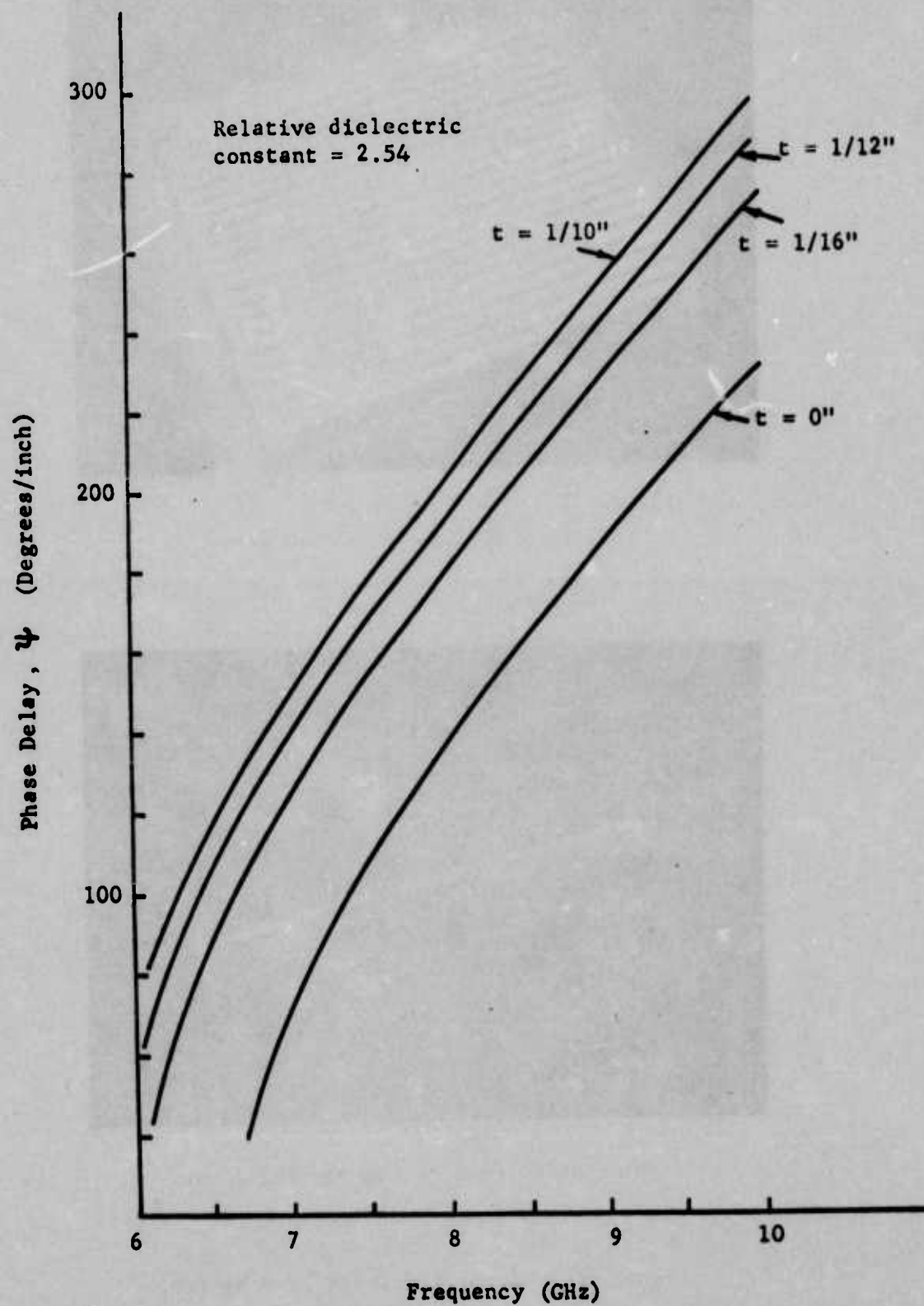
Figure 45. Phase Delay for Dielectric Vane in the Feed System of an N X N Array.

81
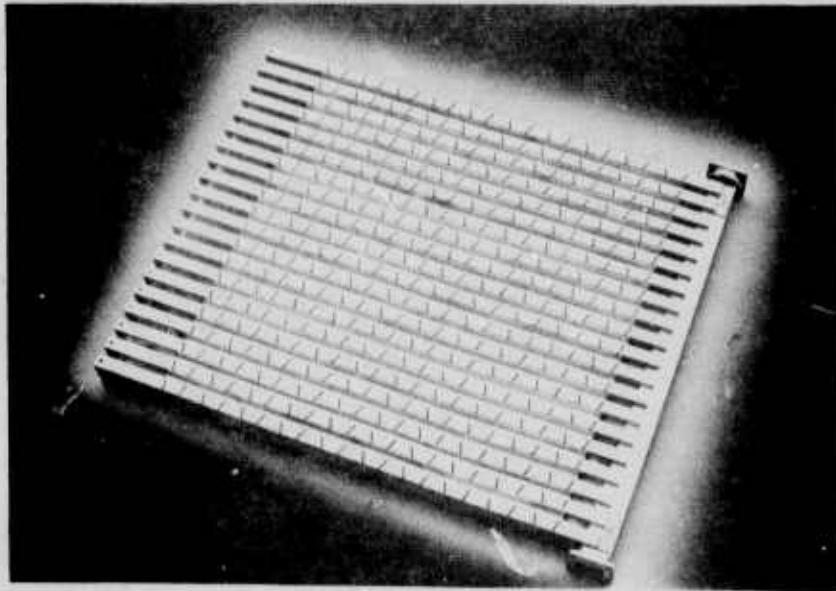
(a) 20 x 20 Element planar array.
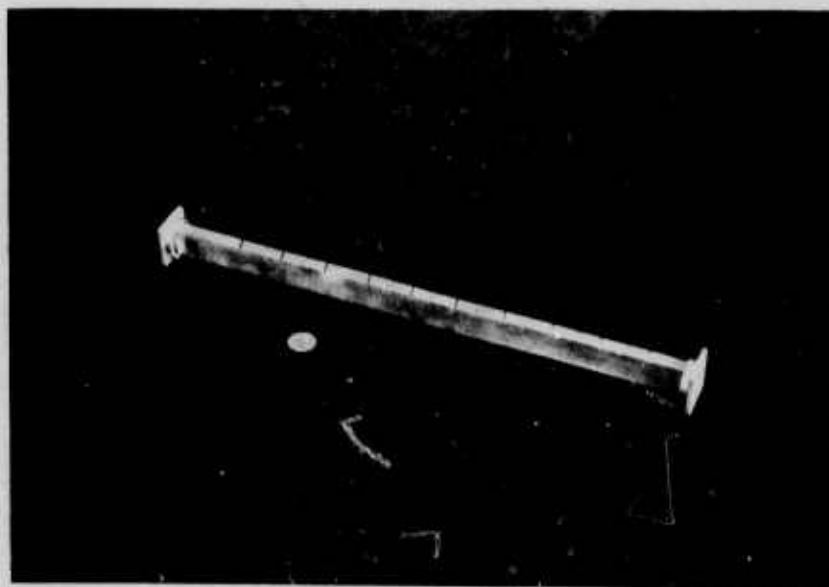
(b) Slotted feed system for the array.

Figure 46. Planar Array for Feed System.

TABLE 4

COMPARISON OF EXPERIMENTAL AND THEORETICAL RESULTS FOR THE BEAM POINTINGS OF A DIELECTRICALLY LOADED SLOTTED WAVEGUIDE SECTION (t = 1/16 inch and ε_r = 2.54)

INSERTION DEPTH (inches)	FREQUENCY (GHz)	THEORETICAL BEAM POINTING (Deg)	EXPERIMENTAL BEAM POINTING (Deg)
0.0	8.5	103.6	103.3
0.2	8.5	---	96.6
0.4	8.5	91.5	92.4
0.0	9.5	93.3	92.7
0.2	9.5	---	87.0
0.4	9.5	81.6	81.9

the feed system can be obtained by controlling the depth of the vane with cams driven by synchronous electric motors contolled by a master time base unit (TBU). The frequency scan of the VCO can be controlled by the TBU in a predetermined sequence with the vane position. By control of the VCO frequency and vane position, non-linear scans can be generated (e.g., conical scans).

The use of the 20 x 20 array in the system will require the use of only one channel in the r-f section. In this configuration, the azimuth beam pointing of the antenna will be controlled by the frequency. The elevation beam pointing will be controlled by the mechanically positioned dieletric vane. Since the antenna array has a gain of 25 dB, the overall antenna gain will be increased by approximately 10 dB over that of the dual beam configuration.

The use of the 400-element array will require the redesign of the multiplexed integration network and the digital detection network. The use of a microcomputer in controlling the entire system will be of primary importance in exploiting the versatility of the scanning antenna.

The objective of the work effort on this phase of the program has been to demonstrate the frequency-mechanical method of scanning the 400-element planar array. The complete design and construction of the TBU, multiplexed integration network, digital detection network, and the overall control by use of a microcomputer have been proposed for a future project.

SECTION V

CONCLUSIONS AND RECOMMENDATIONS

1. CONCLUSIONS

The basic goals set forth in the program were met. In the flight test program for the radiometric bomb guidance system (Martin-Marietta Corporation, Orlando, Florida), the flight tests performed at Orlando, Florida, were successful as a preliminary system testing and evaluation for the joint USAF/Navy helicopter flight test program conducted at Santa Ana, California.

Development of three system configurations were pursued. On the first system, the DBFSR, the following modifications to the original frequency-scanned radiometer greatly enhanced operational performance:

(a) Replacement of the transistor/varactor multiplier voltage controlled oscillator (VCO) frequency source by a varactor tuned Gunn oscillator resulted in the rise time for the frequency shift being improved an order of magnitude.

(b) Redesign of the digital-to-analog (D/A) circuitry greatly improved the drive capability of the VCO tuning voltage network. This is essential for proper operation in the stairstep mode.

(c) The demultiplexer/multiplexer and the integrator network performed satisfactorily for each antenna beam pointing step.

(d) The design and construction of longitudinal shunt-slot array offered an improvement over the original frequency scanned design by generating identical polarizations in each fan beam. Like polarizations are desirable because previous measurements have shown that complex target signatures are dependent on antenna polarization. This enhances target recognition capability in clutter and multiple target situations.

The tower tests for the DBFSR indicated that several improvements were needed to further enhance the target detection capability. The following improvements led to the investigation of a second system design, the MDBFSR:

(a) Incorporation of a range gate circuitry to avoid clutter capture.

(b) A single receiver configuration that time-shares the azimuth and elevation channels, eliminating the requirements for two receivers and resulting in equal signal return for both azimuth and elevation scans.

85

In the third system, the SCDSR, the dual beam antenna of the MDBFSR is replaced by an N x N array that is frequency scanned in azimuth, while being mechanically scanned in elevation by a mechanical phase shifter. Preliminary tests indicate that this antenna configuration performs satisfactorily. The use of this array increases the overall antenna gain and makes possible various scanning modes, such as a conical scan.

2. RECOMMENDATIONS

The following recommendations are made as a result of this program:

(a) Further work should continue on evaluating the MDBFSR.

(b) Development should continue on the SCDSR since this design offers the more versatile scanning capability.

(c) Recent advancement in strip line radiators, using active substrates, makes possible the development of a two dimensional voltage controlled phased array. This revolutionary method of phase scanning should be pursued for adaptation to the SCDSR configuration.

(d) Continued measurements should be made by the Air Force Armament Laboratory to include attenuation as a result of rainfall over the narrow, close-in coordinator as scanned by the radiometer seeker.

INITIAL DISTRIBUTION

AFAL/TE	1	USACDC/CDCCOMSD-D	1
AFAL/TEL	1	USA Electronics Comd (AMSEL-	
AFAL/TEM	1	HL-CT-R)	1
AFAL/NVA	1	General Dynamics (Pomona Div)	1
AFAL/NV	1	Aerojet Electrosystems Co	1
ASD/SD	2	Martin-Marietta Aerospace	2
ASD/ENYS	1	Sperry Microwave Electronic Div	1
RADC/IRA	1	Lockheed Missiles & Space Co	1
6585TG/TD	1	Ballistic Research Labs (AMXBR-	
AUL/AUL-LSE-70-239	1	CA)	1
ATC/XPOS	1	USAF/SAMI	1
ADWC/TEOP	1	AFWL/LR	2
ADWC/4750TS (TEJ)	1	NWC (Code 3542)	1
Naval Weapons Lab (Code FGR/HOYE)	1	DARPA/Director of Sensor	1
ODDR&E/TST&E	1	AFAL/NVA-679A	1
DARPA/TIO	1	Honeywell Systems & Research	1
Navair Sys Comd (AIR 360)	1	Vought Missiles & Space Co	1
Univ of Mich Willow Runs Labs		Motorola	1
(Infrared Info & Analysis Ctr)	1	Louisiana State University	1
Applied Research Lab (Aerospace		The Singer Co	1
Tech Div)	1	AFAL/NVA-698DF	1
Commander, NWC VX-5 (Code 9020)	1	ASD/ENYEHM	1
Commander, NWC (Code 143)	1	Ogden ALC/MMNOP	2
Commander, NWC (Code 352)	1	AFIS/INTA	1
Commander, NWC (Code 4051)	1		
Commander, NWC (Code 753)	1		
Redstone Sci Info Cen (Ch Documents)	2		
Commander, USN Weapons Lab (MAL)	1		
USACDC Coms Gp	1		
USACDC FA Agency	1		
DDC	2		
USACDC (CDCMS-I)	1		
USACDC AVN	1		
ADTC/PP	1		
ADTC/TGW	1		
ADTC/TGWN	1		
ADTC/TGY	1		
TAWC/DT	1		
TAWC/FTS	1		
AFATL/DL	1		
AFATL/DLB	1		
AFATL/DLMM	10		
AFATL/DLOSL	2		
AFATL/DLT	1		
CDCLO/ADTC-SO	1		
TAWC/TRADOCLO	1		
USAMC/AMSMI-RER	2		

(The reverse of this page is blank)